Available online at www.sciencedirect.com
ScienceDirect
Journal of Sound and Vibration 315 (2008) 486–508
JOURNAL OF SOUND AND VIBRATION
www.elsevier.com/locate/jsvi

Analytical and experimental investigations of an autoparametric beam structure

J. Warminski[a,*], M.P. Cartmell[b], M. Bochenski[a], Ivelin Ivanov[c,d]

[a]Department of Applied Mechanics, Lublin University of Technology, Nadbystrzycka 36, 20-618 Lublin, Poland
[b]Mechanical Engineering Department, University of Glasgow, Glasgow, UK
[c]Faculty of Civil and Sanitary Engineering, Lublin University of Technology, Poland
[d]Department of Engineering Mechanics, University of Rousse, Bulgaria

Accepted 14 January 2008
The peer review of this article was organised by the Guest Editor
Available online 5 March 2008

Abstract

This paper discusses theoretical and experimental investigations of vibrations of an autoparametric system composed of two beams with rectangular cross sections. Different flexibilities in the two orthogonal directions are the specific features of the structure. Differential equations of motion and associated boundary conditions, up to third-order approximation, are derived by application of the Hamilton principle of least action. Experimental response of the system, tuned for the 1:4 internal resonance condition, are performed for random and harmonic excitations. The most important vibration modes are extracted from a real mechanical system. It is shown that certain modes in the stiff and flexible directions of both beams may interact, and, intuitively unexpected out-of-plane motion may appear. Preliminary numerical calculations, based on the mathematical model, are also presented.

1. Introduction

Beam structures are common in mechanical and civil engineering [1,2]. Linear and nonlinear models of a single beam have been studied extensively in many papers. Large vibrations of non-planar motion of un-extendable beams are considered in Ref. [3]. Equation of motions with nonlinear curvatures and nonlinear inertia terms are derived systematically up to the third-order approximation, taking bending about two principal axes and torsion of the beam into account. The reduction of the model to two differential equations is carried out by expressing twisting of the beam versus bending in two directions. The response of such a nonlinear model, when excited harmonically by an external distributed force, is presented in Ref. [4]. Paper [5] presents the influence of parametric excitation on a single vertical beam response generated in a perpendicular plane to that of the excitation. It is shown that a few resonances can be excited simultaneously and that a

*Corresponding author. Tel.: +48 81 5384197; fax: +48 81 5384205.
E-mail addresses: j.warminski@pollub.pl (J. Warminski), m.cartmell@mech.gla.ac.uk (M.P. Cartmell), m.bochenski@pollub.pl (M. Bochenski), i.ivanov@pollub.pl (I. Ivanov).
URL: http://www.warminski.pollub.pl (J. Warminski).

0022-460X/$ - see front matter
doi:10.1016/j.jsv.2008.01.048

weaker type of coupling can modify that of stronger coupling to a significant extent. Non-planar motion of a metal cantilever beam excited by vertical harmonic motion of the support is also presented in Ref. [6]. Bifurcation analyses show different possible vibrations of the beam and five branches of the dynamic solution. Periodic, quasi-periodic and chaotic motions are found near the main parametric resonance. Because of a well separated torsional frequency, the influence of torsional inertia is neglected in the model. A study of nonlinear vibrations of metallic cantilever beams subjected to transverse harmonic excitations is given in Ref. [7], where experimental and theoretical results are presented. The energy transfer between widely spaced modes via modulation, both, in the presence and absence, of a one-to-one internal resonance is shown. Reduced-order models using the Galerkin discretisation method are also developed to predict observed experimental motions.

More complicated situation may appear when instead of a single beam, a set of coupled beams is to be analysed. Due to internal coupling, caused by nonlinear terms resulting from nonlinear geometry and inertia, autoparametric vibrations may appear [8]. In such a case, one subsystem becomes a source of excitation for the other, and under some conditions it may lead to an increase in vibration amplitude and, moreover, an energy transfer between different vibration modes [9]. This kind of coupling appears in, so-called, “L” shaped beam structures. In-plane motion analysis of such coupled beams is presented in Ref. [10]. Derivation of the equations of motion and dynamical boundary condition are shown there for a structure flexible in one vertical plane and stiff in the orthogonal direction. Analytical solutions are found in the neighbourhood of the principal parametric resonance and for a 2:1 internal resonance, when the strongest coupling takes place. Primary resonance of the first and the second mode, and prediction of the Hopf bifurcation, are determined analytically. Experimental tests of nonlinear motion in a coupled beam structure with quadratic nonlinearities are discussed in Refs. [11,12]. Periodic, quasi-periodic, and chaotic responses, predicted by theory are confirmed experimentally. It is shown that under the 2:1 internal resonance, a very small excitation can lead to chaotic response of the structure.

Another type of the “L” shaped metal beam structure is explored in Refs. [13–18]. The difference between this and the models just summarised is that the beams are coupled in such a way that their stiffnesses are essentially different in two orthogonal directions (see Fig. 1). The effect of nonlinear coupling between bending modes of vibration is investigated theoretically and experimentally in Refs. [13,14]. The nonlinear forced vibration responses show jumps at entry and exits frequencies. Small nonlinear interactions have significant effect under the 2:1 internal resonance condition. A four-mode interaction exhibits large amplitudes of indirectly excited modes and saturation of the directly excited mode. Planar and non-planar motions of the vertical beam for two simultaneous internal resonance conditions are presented in Ref. [15]. The combination and internal resonances give complicated responses and intermodal energy exchange effects, for small changes in external and internal tuning. Differential equations of motion have been derived taking into account bending of the horizontal beam, and bending/torsion of the vertical beam. It is shown in Ref. [16] that violent non-synchronous torsion and bending vibrations occur as a result of the existence of quadratic nonlinear coupling terms, and internal resonance effects caused by strong four-mode interactions.

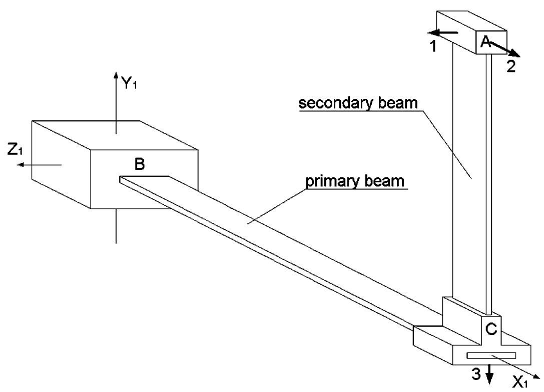

Fig. 1. Model of the structure.

In spite of extensive investigations of the "L" shaped beam structure, there are no literature analyses, to the authors' knowledge, that take interaction between torsion and bending in both of the coupled beams into account. The development of the mathematical modelling is particularly important if the structure is made of composite material. Additional interactions of the composite structure can be observed because of a natural closeness of the torsional and bending mode frequencies, which are usually well separated for metallic structures.

This paper gives an extension of the analysis of the coupled beam structure presented in papers [13–18]. The systematic derivation of the differential equations of motions and associated boundary conditions up to the third-order approximation are given in the first part. Then, the results of preliminary experimental tests and numerical simulations for out-of-plane motion, the modal interactions and their influence on the structure's response phenomena are presented in the second part.

2. Model of the structure

The structure considered in this paper consists of two slender glass epoxy composite beams with reinforcing fibres orientated in the directions given by 0/90/45/–45/45/90/0 (Fig. 1). Both beams are of rectangular cross-section and are fixed in such a way that their flexibilities are essentially different in the horizontal and vertical directions [18]. They are clamped together at point C, while the horizontal (*primary*) beam is fixed at the support B and can be excited by a shaker in the Y_1 direction. A lumped mass A attached at the top of the vertical (*secondary*) beam allows for tuning of the structure for the required dynamical conditions.

The deformed structure and the assumed coordinate systems are presented in Fig. 2. The axes X_1, Y_1, Z_1 are assumed to be inertial with their origin at point B, while the set X_2, Y_2, Z_2 is attached to the centre of the cross-section at point C and overlaps the principal axes of the beam cross-section. Frames ξ_1, η_1, ζ_1 and ξ_2, η_2, ζ_2 are the principal axes of the beam cross-section at arbitrary positions s_1 and s_2 for the primary and secondary beams, respectively. The components $u_1(s_1,t)$, $v_1(s_1,t)$, $w_1(s_1,t)$ and $u_2(s_2,t)$, $v_2(s_2,t)$, $w_2(s_2,t)$ denote the elastic displacement of the cross-section centres of the primary and secondary beams (points O_1 and O_2) in the X_1, Y_1, Z_1 and X_2, Y_2, Z_2 coordinate sets, respectively, while $\phi_1(s_1,t)$, $\psi_1(s_1,t)$, $\theta_1(s_1,t)$ and $\phi_2(s_2,t)$, $\psi_2(s_2,t)$, $\theta_2(s_2,t)$ represent the rotations expressed by the Euler angles.

3. Equations of motion

The equations of free vibration of the structure given in Fig. 1 are derived by applying Hamilton's principle of least action,

$$\delta\int_{t_1}^{t_2}(T_1 - V_1 + F_1 + T_2 - V_2 + F_2 + T_C - V_C + T_A - V_A)\,\mathrm{d}t = 0, \tag{1}$$

where T_1, V_1, F_1, T_2, V_2, F_2 denote the kinetic and potential energies and the constraint equations of the primary and the secondary beams, and T_C, V_C, T_A, V_A, the kinetic and potential energies of the masses C and A, respectively.

By introducing the notation $T_1 - V_1 + F_1 = \int_0^{l_1} h_1\,\mathrm{d}s_1$, $T_2 - V_2 + F_2 = \int_0^{l_2} h_2\,\mathrm{d}s_2$, Eq. (1) can then be re-written in the form

$$\int_{t_1}^{t_2}\left(\int_0^{l_1}\delta h_1\,\mathrm{d}s_1 + \int_0^{l_2}\delta h_2\,\mathrm{d}s_2 + T_C - V_C + T_A - V_A\right)\mathrm{d}t = 0. \tag{2}$$

The kinetic energy of the primary beam results from translational and rotational motions of the element shown in Fig. 2a

$$T_1 = \frac{1}{2}\int_0^{l_1}\left(\rho_1 A_1\left(V_{x_1}^2 + V_{y_1}^2 + V_{z_1}^2\right) + I_{\xi_1}\omega_{\xi_1}^2 + I_{\eta_1}\omega_{\eta_1}^2 + I_{\zeta_1}\omega_{\zeta_1}^2\right)\mathrm{d}s_1, \tag{3}$$

where ρ_1, A_1 denote density and cross-sectional area of the primary beam, and $I_{\xi 1}, I_{\eta 1}, I_{\zeta 1}$ are the principal mass moments of inertia of the beam per unit length. Velocity components of the translational motion take the

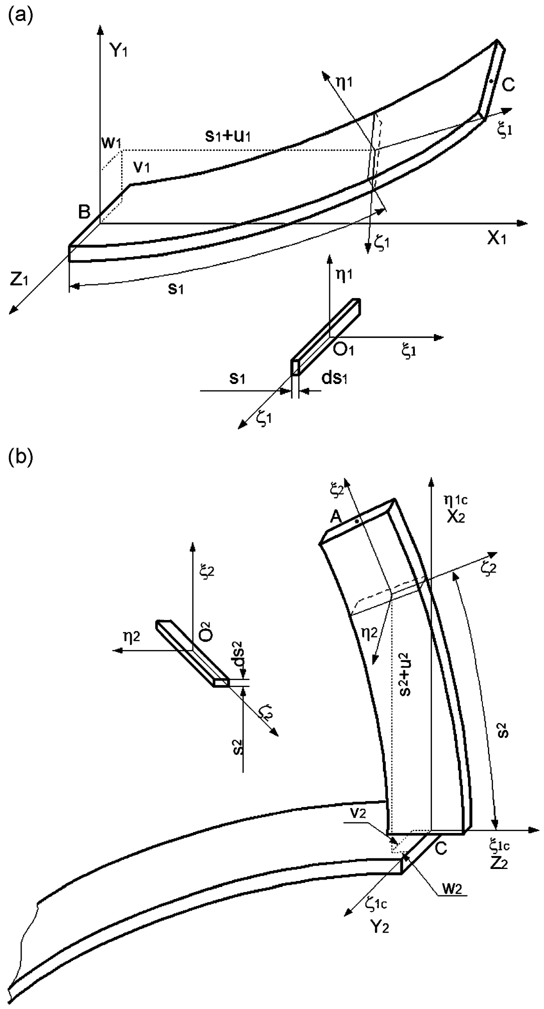

Fig. 2. Deflected beam structure: (a) primary beam and (b) secondary beam.

form

$$V_{x_1} = \dot{u}_1, \quad V_{y_1} = \dot{v}_1, \quad V_{z_1} = \dot{w}_1, \tag{4}$$

where the dot denotes the time derivative. Assuming that the beam is un-extendable, and that there is no shear deformation, we can express θ_1 and ψ_1 versus deformations u_1, v_1, w_1, and then angular velocities can be determined from the rotation of the cross-section which, after expanding of the trigonometric functions in power series, gives [3]

$$\begin{aligned}
\omega_{\xi_1} &= \dot{\phi}_1 + \dot{v}_1' w_1', \\
\omega_{\eta_1} &= \phi_1 \dot{v}'_1 - \dot{w}'_1 + \tfrac{1}{2}\phi_1^2 \dot{w}'_1 - \tfrac{1}{2} w'^2_1 \dot{w}'_1, \\
\omega_{\zeta_1} &= \dot{v}'_1 - \tfrac{1}{2}\phi_1^2 \dot{v}'_1 + \tfrac{1}{2} v'^2_1 \dot{v}'_1 + \phi_1 \dot{w}_1' + v_1' w_1' \dot{w}'_1,
\end{aligned} \tag{5}$$

where the prime denotes the space derivative.

Taking into account the geometry of the beam of Fig. 2(a), we can assume that the angular velocity with respect to the η_1 axis, and the mass moment of inertia relative to the ζ_1 axis, are relatively small, therefore,

$$\omega_{\eta_1}^2 \cong 0, \quad I_{\zeta_1} \cong 0.$$

Thus we keep only that part of the kinetic energy that corresponds to rotation with respect to the ξ_1 axis:

$$\omega_{\xi_1} = \dot{\phi}_1 + \dot{v}'_1 w'_1. \tag{6}$$

Potential energy is determined in bending about the two principal axes η_1, ζ_1, and in torsion about axis ξ_1,

$$V_1 = \frac{1}{2}\int_0^{l_1} \left(D_{\xi_1}\rho^2_{\xi_1} + D_{\eta_1}\rho^2_{\eta_1} + D_{\zeta_1}\rho^2_{\zeta_1} \right) \mathrm{d}s_1, \tag{7}$$

where $D_{\xi_1} = G_1 J_{\xi_1}$ means the torsional stiffness, $D_{\eta_1} = E_1 J_{\eta_1}$, $D_{\zeta_1} = E_1 J_{\zeta_1}$ flexural stiffnesses and $\rho_{\xi 1}, \rho_{\eta 1}, \rho_{\zeta 1}$ are the curvatures, determined from the angular velocities by using Kirchhoff's kinetic analogue [6]:

$$\begin{aligned} \rho_{\xi_1} &= \phi'_1 + w'_1 v''_1, \\ \rho_{\eta_1} &= \phi_1 v''_1 - w''_1 + \tfrac{1}{2}\phi_1^2 w''_1 - \tfrac{1}{2} w'^2_1 w''_1, \\ \rho_{\zeta_1} &= v''_1 - \tfrac{1}{2}\phi_1^2 v''_1 + \tfrac{1}{2} v'^2_1 v''_1 + \phi_1 w''_1 + v'_1 w'_1 w''_1. \end{aligned} \tag{8}$$

The constraint equation for the primary beam has the form,

$$F_1 = \int_0^{l_1} \lambda_1 (1 - ((1 + u'_1)^2 + v'^2_1 + w'^2_1))\, \mathrm{d}s_1, \tag{9}$$

where λ_1 is the Lagrange multiplier.

The kinetic energy of the secondary beam is calculated by taking into account the velocity $\mathbf{V}_{O_2}$ of the centre of the cross-section O_2, related to the translational and angular motions of set $X_2Y_2Z_2$ which has its origin at point C, together with the relative velocity $\mathbf{V}_r$. It can be written in vector form,

$$\mathbf{V}_{O_2} = \mathbf{V}_C + \boldsymbol{\omega}_{C2} \times \mathbf{r}_2 + \mathbf{V}_r, \tag{10}$$

where $\mathbf{r}_2 = [u_2,\ v_2,\ w_2]$.

Applying, and then projecting the velocity components onto the $X_2Y_2Z_2$ coordinate set we get the kinetic energy of the secondary beam,

$$T_2 = \frac{1}{2}\int_0^{l_2} \left(\rho_2 A_2 \left(V^2_{x_2} + V^2_{y_2} + V^2_{z_2} \right) + I_{\xi_2}\omega^2_{\xi_2} + I_{\eta_2}\omega^2_{\eta_2} + I_{\zeta_2}\omega^2_{\zeta_2} \right) \mathrm{d}s_2. \tag{11}$$

Absolute velocity components projected onto the moving frame take the forms

$$\begin{aligned} V_{x_2} &= \dot{u}_2 + \phi_{1C}\dot{w}_{1C} - v_2(\dot{\phi}_{1C} + \dot{v}'_{1C} w'_{1C}) - w_2(\dot{v}'_{1C} + \phi_{1C}\dot{w}_{1C}) + \dot{v}_{1C}\left(1 - \tfrac{1}{2}\phi^2_{1C} - \tfrac{1}{2} v'^2_{1C}\right) \\ &\quad + \dot{u}_{1C}(-v'_{1C} - \phi_{1C} w'_{1C}), \\ V_{y_2} &= \dot{v}_2 + (s_2 + u_2)(\dot{\phi}_{1C} + \dot{v}'_{1C} w'_{1C}) + w_2(\phi_{1C}\dot{v}'_{1C} - \dot{w}'_{1C}) + \dot{u}_{1C}(\phi_{1C} v'_{1C} - w'_{1C}) \\ &\quad + \dot{v}_{1C}(-\phi_{1C} - v'_{1C} w'_{1C}) + \dot{w}_{1C}\left(1 - \tfrac{1}{2}\phi^2_{1C} - \tfrac{1}{2} w'^2_{1C}\right), \\ V_{z_2} &= \dot{w}_2 - (s_2 + u_2)(\dot{v}'_{1C} + \phi_{1C}\dot{w}'_{1C}) + s_2\left(\tfrac{1}{2}\phi^2_{1C}\dot{v}'_{1C} - \tfrac{1}{2}\dot{v}'_{1C} v'^2_{1C} - \dot{w}'_{1C} v'_{1C} w'_{1C}\right) \\ &\quad + v_2(\phi_{1C}\dot{v}'_{1C} - \dot{w}'_{1C}) + \dot{v}_{1C} v'_{1C} + \dot{w}_{1C} w'_{1C} + \dot{u}_{1C}\left(1 - \tfrac{1}{2} v'^2_{1C} - \tfrac{1}{2} w'^2_{1C}\right). \end{aligned} \tag{12}$$

Making assumptions similar to those of the primary beam,

$$\omega^2_{\eta_2} \cong 0, \quad I_{\zeta_2} \cong 0,$$

we get

$$\omega_{\xi_2} = \dot{\phi}_2 + \dot{v}'_2 w'_2. \tag{13}$$

The potential energy of the secondary beam is expressed in the second local coordinate set, denoted by index 2, and has an equivalent form to that of the primary beam,

$$V_2 = \frac{1}{2}\int_0^{l_2} \left(D_{\xi_2}\rho^2_{\xi_2} + D_{\eta_2}\rho^2_{\eta_2} + D_{\zeta_2}\rho^2_{\zeta_2} \right) \mathrm{d}s_2 \tag{14}$$

with torsional and flexural stiffnesses,

$$D_{\xi_2} = G_2 J_{\xi_2}, \quad D_{\eta_2} = E_2 J_{\eta_2}, \quad D_{\zeta_2} = E_2 J_{\zeta_2}$$

and curvatures

$$\begin{aligned} \rho_{\xi_2} &= \phi_2' + w_2' v_2'', \\ \rho_{\eta_2} &= \phi_2 v_2'' - w_2'' + \tfrac{1}{2}\phi_2^2 w_2'' - \tfrac{1}{2} w_2'^2 w_2'', \\ \rho_{\zeta_2} &= v_2'' - \tfrac{1}{2}\phi_2^2 v_2'' + \tfrac{1}{2} v_2'^2 v_2'' + \phi_2 w_2'' + v_2' w_2' w_2''. \end{aligned} \tag{15}$$

The constraint equation for the secondary beam is defined as

$$F_2 = \int_0^{l_2} \lambda_2 (1 - ((1 + u_2')^2 + v_2'^2 + w_2'^2))\, \mathrm{d}s_2. \tag{16}$$

To obtain the differential equations of motion it is necessary to determine the variations of the functions h_1 and h_2, L_A, and L_C,

$$\delta h_1 = \sum_{i=1}^{13} \frac{\partial h_1}{\partial p_i}\, \delta p_i, \quad p = \mathrm{col}\{\phi_1, \dot{u}_1, \dot{v}_1, \dot{w}_1, \dot{\phi}_1, \dot{v}_1', u_1', v_1', w_1', \phi_1', v_1'', w_1'', \lambda_1\}, \tag{17}$$

$$\delta h_2 = \sum_{i=1}^{25} \frac{\partial h_2}{\partial q_i}\, \delta q_i, \quad \begin{aligned} q = \mathrm{col}\{& u_2, v_2, w_2, \phi_2, \dot{u}_2, \dot{v}_2, \dot{w}_2, \dot{\phi}_2, \dot{v}_2', u_2', v_2', w_2', \phi_2', v_2'', w_1'', \\ & \lambda_2, \phi_{1C}, \dot{u}_{1C}, \dot{v}_{1C}, \dot{w}_{1C}, \dot{\phi}_{1C}, v_{1C}', w_{1C}', \dot{v}_{1C}', \dot{w}_{1C}'\}, \end{aligned} \tag{18}$$

$$\delta L_C = \sum_{i=1}^{10} \frac{\partial L_C}{\partial p_{Ci}}\, \delta p_{Ci}, \quad p_C = \mathrm{col}\{v_1, \phi_1, \dot{u}_1, \dot{v}_1, \dot{w}_1, \dot{\phi}_1, v_1', w_1', \dot{v}'_1, \dot{w}'_1\}, \tag{19}$$

$$\delta L_A = \sum_{i=1}^{21} \frac{\partial L_A}{\partial q_{Ai}}\, \delta q_{Ai}, \quad \begin{aligned} q_A = \mathrm{col}\{& u_2, v_2, w_2, \phi_2, \dot{u}_2, \dot{v}_2, \dot{w}_2, \dot{\phi}_2, \dot{v}_2', \dot{w}_2', v_2', \\ & w_2', \phi_{1C}, \dot{u}_{1C}, \dot{v}_{1C}, \dot{w}_{1C}, \dot{\phi}_{1C}, v_{1C}', w_{1C}', \dot{v}_{1C}', \dot{w}_{1C}'\}. \end{aligned} \tag{20}$$

Next, integrating by parts with respect to time limits t_1 and t_2, and remembering that variations at the time instances t_1 and t_2 are equal to zero we get,

$$\begin{aligned} \int_{t_1}^{t_2} \Bigg\{ & \int_0^{l_1} \Bigg[\left(-\frac{\partial^2 h_1}{\partial \dot{u}_1 \partial t} - \frac{\partial^2 h_1}{\partial u_1' \partial s_1} \right) \delta u_1 + \left(-\frac{\partial^2 h_1}{\partial \dot{v}_1 \partial t} + \frac{\partial^3 h_1}{\partial \dot{v}_1' \partial s_1 \partial t} - \frac{\partial^2 h_1}{\partial v_1' \partial s_1} + \frac{\partial^3 h_1}{\partial v_1'' \partial s_1^2} \right) \delta v_1 \\ & + \left(-\frac{\partial^2 h_1}{\partial \dot{w}_1 \partial t} - \frac{\partial^2 h_1}{\partial w_1' \partial s_1} + \frac{\partial^3 h_1}{\partial w_1'' \partial s_1^2} \right) \delta w_1 + \left(\frac{\partial h_1}{\partial \phi_1} - \frac{\partial^2 h_1}{\partial \dot{\phi}_1 \partial t} - \frac{\partial^2 h_1}{\partial \phi_1' \partial s_1} \right) \delta \phi_1 + \frac{\partial h_1}{\partial \lambda_1} \delta \lambda_1 \Bigg] \mathrm{d}s_1 \\ & + \int_0^{l_2} \Bigg[\left(\frac{\partial h_2}{\partial u_2} - \frac{\partial^2 h_2}{\partial \dot{u}_2 \partial t} - \frac{\partial^2 h_2}{\partial u_2' \partial s_2} \right) \delta u_2 + \left(\frac{\partial h_2}{\partial v_2} - \frac{\partial^2 h_2}{\partial \dot{v}_2 \partial t} + \frac{\partial^3 h_2}{\partial \dot{v}_2' \partial s_2 \partial t} - \frac{\partial^2 h_2}{\partial v_2' \partial s_2} + \frac{\partial^3 h_2}{\partial v_2'' \partial s_2^2} \right) \delta v_2 \\ & + \left(\frac{\partial h_2}{\partial w_2} - \frac{\partial^2 h_2}{\partial \dot{w}_2 \partial t} - \frac{\partial^2 h_2}{\partial w_2' \partial s_2} + \frac{\partial^3 h_2}{\partial w_2'' \partial s_2^2} \right) \delta w_2 + \left(\frac{\partial h_2}{\partial \phi_2} - \frac{\partial^2 h_2}{\partial \dot{\phi}_2 \partial t} - \frac{\partial^2 h_2}{\partial \phi_2' \partial s_2} \right) \delta \phi_2 + \frac{\partial h_2}{\partial \lambda_2} \delta \lambda_2 \Bigg] \mathrm{d}s_2 \Bigg\} \mathrm{d}t = 0. \end{aligned} \tag{21}$$

From that point, integrating by parts with respect to the space coordinates s_1 and s_2, and then collecting terms for proper variations, up to the third order, we get successive differential equations of motions:

- for the primary beam
  variation δu_1

$$-\rho_1 A_1 \ddot{u}_1 + \lambda_1 u_1'' = 0, \tag{22}$$

variation δv_1

$$-\rho_1 A_1 \ddot{v}_1 + \lambda_1 v_1'' + D_{\xi 1}(-\phi_1''' w_1' - v_1^{\mathrm{IV}} w_1'^2 - w_1'''(\phi_1' + 2w_1' v_1'') - 2w_1''(2v_1''' w_1' + v_1'' w_1'' + \phi_1''))$$
$$+ D_{\eta 1}(w_1^{\mathrm{IV}}\phi_1 - v_1^{\mathrm{IV}}\phi_1^2 + 2w_1'''\phi_1' - 4v_1'''\phi_1\phi_1' - 2v_1''(\phi_1'^2 + \phi_1\phi_1'') + w_1''\phi_1'')$$
$$+ D_{\zeta 1}(-v_1^{\mathrm{IV}}(1 - \phi_1^2 + v_1'^2) - w_1^{\mathrm{IV}}(\phi_1 + v_1' w_1') + 4v_1'''(\phi_1\phi_1' - v_1' v_1'') - w_1'''(2\phi_1' + w_1' v_1'' + 3v_1' w_1'')$$
$$+ v_1''(2\phi_1'^2 - v_1''^2 - w_1''^2 + 2\phi_1\phi_1'') - w_1''\phi_1'') + I_1(\dot{w}_1'\dot{\phi}_1' + w_1'(\ddot{\phi}_1' + 2\dot{w}_1'\dot{v}_1'' + w_1'\ddot{v}_1'' + 2\dot{v}_1'\dot{w}_1'')$$
$$+ w_1''(\ddot{\phi}_1 + 2w_1'\ddot{v}_1' + 2\dot{v}_1'\dot{w}_1') + \dot{\phi}_1\dot{w}_1'') = 0, \tag{23}$$

variation δw_1

$$-\rho_1 A_1 \ddot{w}_1 + \lambda_1 w_1'' + D_{\xi 1}(v_1'''(\phi_1' + 2w_1' v_1'') + v_1''^2 w_1'' + v_1''\phi_1'') + D_{\eta 1}(-w_1^{\mathrm{IV}}(1 - \phi_1^2 + w_1'^2)$$
$$+ v_1^{\mathrm{IV}}\phi_1 + 2v_1'''\phi_1' + 4w_1'''(\phi_1\phi_1' - w_1' w_1'') + w_1''(2\phi_1'^2 - w_1''^2 + 2\phi_1\phi_1'') + v_1''\phi_1'')$$
$$+ D_{\zeta 1}(-v_1^{\mathrm{IV}}(\phi_1 + v_1' w_1') - w_1^{\mathrm{IV}}\phi_1^2 - v_1'''(2\phi_1' + 3w_1' v_1'' + v_1' w_1'') - 4w_1'''\phi_1\phi_1'$$
$$- w_1''(2\phi_1'^2 + v_1''^2 + 2\phi_1\phi_1'') - v_1''\phi_1'') + I_1(-\dot{v}_1'\dot{\phi}_1' - \dot{v}_1'^2 w_1'' - \dot{\phi}_1\dot{v}_1'' - 2w_1'\dot{v}_1'\dot{v}_1'') = 0, \tag{24}$$

variation $\delta\phi_1$

$$D_{\xi 1}(v_1''' w_1' + v_1'' w_1'' + \phi_1'') + D_{\eta 1}(-\phi_1 v_1''^2 + v_1'' w_1'' + \phi_1 w_1''^2)$$
$$+ D_{\zeta 1}(\phi_1 v_1''^2 - v_1'' w_1'' - \phi_1 w_1''^2) + I_1(-\ddot{\phi}_1 - w_1'\ddot{v}_1' - \dot{v}_1'\dot{w}_1') = 0, \tag{25}$$

variation $\delta\lambda_1$

$$(1 - [(1 + u_1')^2 + v_1'^2 + w_1'^2]) = 0. \tag{26}$$

- for the secondary beam
  variation δu_2

$$\rho_2 A_2(-\ddot{u}_2 - \ddot{v}_{1C}\left(1 - \tfrac{1}{2}\phi_{1C}^2 - \tfrac{1}{2}v_{1C}'^2\right) + s_2(\dot{\phi}_{1C}^2 + \dot{v}_{1C}'^2 + 2\phi_{1C}\dot{v}'_{1C}\dot{w}'_{1C} + 2\dot{\phi}_{1C}\dot{v}'_{1C}w'_{1C})$$
$$+ u_2(\dot{\phi}_{1C}^2 + \dot{v}_{1C}'^2) + v_2(\ddot{\phi}_{1C} + \dot{v}_{1C}'^2 + 2\dot{v}'_{1C}\dot{w}'_{1C} + \ddot{v}'_{1C}w'_{1C}) + w_2(\ddot{v}'_{1C} + \phi_{1C}\ddot{w}'_{1C})$$
$$+ 2\dot{v}_2(\dot{\phi}_{1C} + \dot{v}'_{1C}w'_{1C}) + \ddot{u}_{1C}(v'_{1C} + \phi_{1C}w'_{1C}) - \ddot{w}_{1C}\phi_{1C}) + \lambda_2 u_2'' = 0, \tag{27}$$

variation δv_2

$$\rho_2 A_2(-\ddot{v}_2 - \ddot{w}_{1C}\left(1 - \tfrac{1}{2}\phi_{1C}^2 - \tfrac{1}{2}w_{1C}'^2\right) - s_2(\ddot{\phi}_{1C} + \phi_{1C}\dot{v}_{1C}'^2 - \phi_{1C}\dot{w}_{1C}'^2 + \ddot{v}'_{1C}w'_{1C}) - u_2(\ddot{\phi}_{1C} + \ddot{v}'_{1C}w'_{1C})$$
$$+ v_2(\dot{\phi}_{1C}^2 + \dot{w}_{1C}'^2) + w_2\ddot{w}'_{1C} - 2\dot{u}_2(\dot{\phi}_{1C} + \dot{v}'_{1C}w'_{1C}) + \ddot{u}_{1C}(w'_{1C} - \phi_{1C}v'_{1C}) + \ddot{v}_{1C}(v'_{1C}w'_{1C} + \phi_{1C}))$$
$$+ \lambda_2 v_2'' + D_{\xi 2}(-\phi_2''' w_2' - v_2^{\mathrm{IV}} w_2'^2 - w_2'''(\phi_2' + 2w_2' v_2'') - 2w_2''(2v_2''' w_2' + v_2'' w_2'' + \phi_2''))$$
$$+ D_{\eta 2}(w_2^{\mathrm{IV}}\phi_2 - v_2^{\mathrm{IV}}\phi_2^2 + 2w_2'''\phi_2' - 4v_2'''\phi_2\phi_2' - 2v_2''(\phi_2'^2 + \phi_2\phi_2'') + w_2''\phi_2'')$$
$$+ D_{\zeta 2}(-v_2^{\mathrm{IV}}(1 - \phi_2^2 + v_2'^2) - w_2^{\mathrm{IV}}(\phi_2 + v_2' w_2') + 4v_2'''(\phi_2\phi_2' - v_2' v_2'') - w_2'''(2\phi_2' + w_2' v_2'' + 3v_2' w_2'')$$
$$+ v_2''(2\phi_2'^2 - v_2''^2 - w_2''^2 + 2\phi_2\phi_2'') - w_2''\phi_2'') + I_2(\dot{w}_2'\dot{\phi}_2' + w_2'(\ddot{\phi}_2' + 2\dot{w}_2'\dot{v}_2'' + w_2'\ddot{v}_2'' + 2\dot{v}_2'\dot{w}_2'')$$
$$+ w_2''(\ddot{\phi}_2 + 2w_2'\ddot{v}_2' + 2\dot{v}_2'\dot{w}_2') + \dot{\phi}_2\dot{w}_2'') = 0, \tag{28}$$

variation δw_2

$$\rho_2 A_2\Big(-\ddot{w}_2 + s_2\Big(\ddot{v}'_{1C}\left(1 - \tfrac{1}{2}\phi_{1C}^2 + \tfrac{1}{2}v_{1C}'^2\right) + \ddot{w}'_{1C}(\phi_{1C} + v'_{1C}w'_{1C}) + v'_{1C}(\dot{v}_{1C}'^2 + \dot{w}_{1C}'^2)\Big) + u_2(\ddot{v}'_{1C} + \phi_{1C}\ddot{w}'_{1C})$$
$$+ v_2(\ddot{w}'_{1C} - \phi_{1C}\ddot{v}'_{1C}) + w_2(\dot{v}_{1C}'^2 + \dot{w}_{1C}'^2) + 2\dot{u}_{1C}(\dot{v}'_{1C}v'_{1C} + \dot{w}'_{1C}w'_{1C}) - 2\dot{v}_{1C}\dot{v}'_{1C} - 2\dot{w}_{1C}\dot{w}'_{1C}$$
$$-\ddot{u}_{1C}\left(1 - \tfrac{1}{2}v_{1C}'^2 - \tfrac{1}{2}w_{1C}'^2\right) - \ddot{v}_{1C}v'_{1C} - \ddot{w}_{1C}w'_{1C}\Big) + \lambda_2 w_2'' + D_{\xi 2}(v_2'''(\phi_2' + 2w_2' v_2'') + v_{1C}''^2 w_2'' + v_2''\phi_2'')$$

$$+ D_{\eta 2}(-w_2^{IV}(1-\phi_2^2+w'^2_2)+v_2^{IV}\phi_2+2v_2'''\phi_2'+4w_2'''(\phi_2\phi_2'-w_2'w_2'')$$
$$+ w_2''(2\phi'^2_2-w''^2_2+2\phi_2\phi_2'')+v_2''\phi_2'')+D_{\zeta 2}(-v_2^{IV}\left(\phi_2+v_2'w_2'\right)$$
$$- w_2^{IV}\phi_2^2-v_2'''\left(2\phi_2'+3w_2'v_2''+v_2'w_2''\right)-4w_2'''\phi_2\phi_2'-w_2''(2\phi'^2_2+v''^2_2+2\phi_2\phi_2'')-v_2''\phi_2'')$$
$$+ I_2(-\dot{v}_2'\dot{\phi}_2'-\dot{v}'^2_2w_2''-\dot{\phi}_2\dot{v}_2''-2w_2'\dot{v}_2'\dot{v}_2'')=0, \tag{29}$$

variation $\delta\phi_2$

$$D_{\xi 2}(v_2'''w_2'+v_2''w_2''+\phi_2'')+D_{\eta 2}(-\phi_2v''^2_2+v_2''w_2''+\phi_2w''^2_2)$$
$$+ D_{\zeta 2}(\phi_2v''^2_2-v_2''w_2''-\phi_2w''^2_2)+I_2(-\ddot{\phi}_2-w_2'\ddot{v}_2'-\dot{v}_2'\dot{w}_2')=0, \tag{30}$$

variation $\delta\lambda_2$

$$(1-[(1+u_2')^2+v'^2_2+w'^2_2])=0. \tag{31}$$

The components obtained from integration by parts for the limits $s_1=0$, $s_1=l_1$ and $s_2=0$, $s_2=l_2$, and then grouped for the appropriate variations, give the associated boundary conditions as follows:

- *at point B*, $s_1=0$

$$u_{1B}=0,\quad v_{1B}=0,\quad w_{1B}=0,\quad \phi_{1B}=0,\quad v'_{1B}=0,\quad w'_{1B}=0, \tag{32}$$

- *at point C*, $s_1=l_1$, $s_2=0$
  variation δu_{1C}

$$-\lambda_1(1+u'_{1C})-\rho_2A_2l_2[\ddot{w}_{2A}+\ddot{u}_{1C}-l_2\ddot{v}'_{1C}]-m_C\ddot{u}_{1C}-m_A[\ddot{w}_{2A}+\ddot{u}_{1C}-l_2\ddot{v}'_{1C}]+\mathrm{HOT}=0, \tag{33}$$

variation δv_{1C}

$$D_{\zeta 1}v'''_{1C}-\lambda_1v'_{1C}-\rho_2A_2l_2[\ddot{u}_{2A}+\ddot{v}_{1C}]-m_Cg-m_C\ddot{v}_{1C}-m_Ag-m_A[\ddot{u}_{2A}+\ddot{v}_{1C}]+\mathrm{HOT}=0, \tag{34}$$

variation δw_{1C}

$$D_{\eta 1}w'''_{1C}-\lambda_1w'_{1C}-\rho_2A_2l_2[\ddot{v}_{2A}+\ddot{w}_{1C}+l_2\ddot{\phi}_{1C}]-m_C\ddot{w}_{1C}-m_A[\ddot{v}_{2A}+\ddot{w}_{1C}+l_2\ddot{\phi}_{1C}]+\mathrm{HOT}=0, \tag{35}$$

variation $\delta\phi_{1C}$

$$-D_{\xi 1}\phi'_{1C}-\rho_2A_2l_2[l_2(\ddot{v}_{2A}+\ddot{w}_{1C})+l_2^2\ddot{\phi}_{1C}]-I_{C\xi}\ddot{\phi}_{1C}-m_A[l_2(\ddot{v}_{2A}+\ddot{w}_{1C})+l_2^2\ddot{\phi}_{1C}]$$
$$+ m_Ag(v_{2A}+l_2\phi_{1C})+\mathrm{HOT}=0, \tag{36}$$

variation $\delta v'_{1C}$

$$-D_{\zeta 1}v''_{1C}-\rho_2A_2l_2[-l_2(\ddot{w}_{2A}+\ddot{u}_{1C})+l_2^2\ddot{v}'_{1C}]-I_{C\zeta}\ddot{v}'_{1C}$$
$$-m_A[-l_2(\ddot{w}_{2A}+\ddot{u}_{1C})+l_2^2\ddot{v}'_{1C}]-m_Ag(w_{2A}-l_2v'_{1C})+\mathrm{HOT}=0, \tag{37}$$

variation $\delta w'_{1C}$

$$-D_{\eta 1}w''_{1C}-I_{C\eta}\ddot{w}'_{1C}+\mathrm{HOT}=0. \tag{38}$$

- *at point A*, $s_2=l_2$
  variation δu_{2A}

$$-\lambda_2(1+u'_{2A})-m_Ag-m_A[\ddot{u}_{2A}+\ddot{v}_{1C}]+\mathrm{HOT}=0, \tag{39}$$

variation δv_{2A}

$$D_{\zeta 2}v'''_{2A}-\lambda_2v'_{2A}-m_Ag\phi_{1C}-m_A[\ddot{v}_{2A}+\ddot{w}_{1C}+l_2\ddot{\phi}_{1C}]+\mathrm{HOT}=0, \tag{40}$$

variation δw_{2A}

$$D_{\eta 2} w'''_{2A} - \lambda_2 w'_{2A} - m_A g v'_{1C} - m_A[\ddot{w}_{2A} + \ddot{u}_{1C} - l_2 \ddot{v}'_{1C}] + \text{HOT} = 0, \tag{41}$$

variation $\delta \phi_{2A}$

$$-D_{\xi 2} \phi'_{2A} - I_{A\xi} \ddot{\phi}_{2A} + \text{HOT} = 0, \tag{42}$$

variation $\delta v'_{2A}$

$$-D_{\zeta 2} v''_{2A} - I_{A\zeta} \ddot{v}'_{2A} + \text{HOT} = 0, \tag{43}$$

variation $\delta w'_{2A}$

$$-D_{\eta 2} w''_{2A} - I_{A\eta} \ddot{w}'_{2A} + \text{HOT} = 0. \tag{44}$$

Equations for the boundary conditions are given up to the first-order terms while the second and third orders are written by the abbreviation HOT (higher order terms). Indices A, B and C denote values at the proper points. Note that to have consistency in Eqs. (33)–(38) variations of the secondary beam at point $s_2 = 0$ are expressed by variations of the primary beam at $s_1 = l_1$, by using a transformation of the local to the absolute set of coordinates.

The derived partial differential equations which describe the problem consist of the geometrical and inertial nonlinear terms and nonlinear, non-homogenous, dynamical boundary conditions. To solve this set of nonlinear equations of motion, and the nonlinear boundary conditions, an approximate analytical method has to be applied. It requires an appropriate assumption for the admissible vibration modes which will then satisfy the boundary conditions to the required perturbation order accuracy. However, to make proper assumptions for this further work on an approximate analytical approach, certain experimental and numerical (finite element analysis (FEA)) tests had to be undertaken, and these are presented in the next section.

Determining the Lagrange multipliers and then introducing dimensionless time $\tau = \omega t$, where $\omega = \sqrt{D_{\zeta 1}/\rho_1 A_1 l_1^4}$, and dimensionless coefficients

$$\frac{D_{\xi 1}}{D_{\zeta 1}} = \tilde{D}_{\xi 1}, \quad \frac{D_{\eta 1}}{D_{\zeta 1}} = \tilde{D}_{\eta 1}, \quad \frac{D_{\xi 2}}{D_{\zeta 1}} = \tilde{D}_{\xi 2}, \quad \frac{D_{\eta 2}}{D_{\zeta 1}} = \tilde{D}_{\eta 2}, \quad \frac{D_{\zeta 2}}{D_{\zeta 1}} = \tilde{D}_{\zeta 2},$$
$$\frac{I_{C\xi}}{\rho_1 A_1 l_1^3} = \tilde{I}_{C\xi}, \quad \frac{I_{C\eta}}{\rho_1 A_1 l_1^3} = \tilde{I}_{C\eta}, \quad \frac{I_{C\zeta}}{\rho_1 A_1 l_1^3} = \tilde{I}_{C\zeta}, \quad \frac{I_{A\xi}}{\rho_1 A_1 l_1^3} = \tilde{I}_{A\xi}, \quad \frac{I_{A\eta}}{\rho_1 A_1 l_1^3} = \tilde{I}_{A\eta}, \quad \frac{I_{A\zeta}}{\rho_1 A_1 l_1^3} = \tilde{I}_{A\zeta},$$
$$\frac{a_1^2 + b_1^2}{12 l_1^2} = \tilde{I}_1, \quad \frac{a_2^2 + b_2^2}{12 l_1^2} = \tilde{I}_2, \quad \frac{\rho_2 A_2}{\rho_1 A_1} = \tilde{m}_2, \quad \frac{\rho_2 A_2 l_2}{\rho_1 A_1 l_1} = \tilde{M}_2, \quad \frac{m_A}{\rho_1 A_1 l_1} = \tilde{M}_A, \quad \frac{m_C}{\rho_1 A_1 l_1} = \tilde{M}_C,$$
$$\frac{l_2}{l_1} = \tilde{L}_2, \quad g^* = \frac{g}{\omega^2 l_1} = \frac{g}{D_{\zeta 1}} \rho_1 A_1 l_1^3,$$

we get equations of motions and the boundary conditions in dimensionless form (the "tilde" used for dimensionless parameters definition has been dropped for simplicity):

- v_1 direction

$$\begin{aligned}
&- \ddot{v}_1 + \lambda_1 v''_1 + D_{\xi 1}(-\phi'''_1 w'_1 - v^{IV}_1 w'^2_1 - w'''_1(\phi'_1 + 2w'_1 v''_1) - 2w''_1(2v'''_1 w'_1 + v''_1 w''_1 + \phi''_1)) \\
&+ D_{\eta 1}(w^{IV}_1 \phi_1 - v^{IV}_1 \phi^2_1 + 2w'''_1 \phi'_1 - 4v'''_1 \phi_1 \phi'_1 - 2v''_1(\phi'^2_1 + \phi_1 \phi''_1) + w''_1 \phi''_1) \\
&+ (-v^{IV}_1(1 - \phi^2_1 + v'^2_1) - w^{IV}_1(\phi_1 + v'_1 w'_1) + 4v'''_1(\phi_1 \phi'_1 - v'_1 v''_1) - w'''_1(2\phi'_1 + w'_1 v''_1 + 3v'_1 w''_1) \\
&+ v''_1(2\phi'^2_1 - v''^2_1 - w''^2_1 + 2\phi_1 \phi''_1) - w''_1 \phi''_1) + I_1(\dot{w}'_1 \dot{\phi}'_1 + w'_1(\ddot{\phi}'_1 + 2\dot{w}'_1 \dot{v}''_1 + w'_1 \ddot{v}''_1 + 2\dot{v}'_1 \dot{w}''_1) \\
&+ w''_1(\ddot{\phi}_1 + 2w'_1 \ddot{v}'_1 + 2\dot{v}'_1 \dot{w}'_1) + \dot{\phi}_1 \dot{w}''_1) = 0,
\end{aligned} \tag{45}$$

- w_1 direction

$$
\begin{aligned}
&-\ddot{w}_1+\lambda_1 w_1''+D_{\xi 1}(v_1'''(\phi_1'+2w_1'v_1'')+v''^2_1 w_1''+v_1''\phi_1'')\\
&+D_{\eta 1}(-w_1^{\mathrm{IV}}(1-\phi_1^2+w'^2_1)+v_1^{\mathrm{IV}}\phi_1+2v_1'''\phi_1'+4w_1'''(\phi_1\phi_1'-w_1'w_1'')+w_1''(2\phi'^2_1-w''^2_1+2\phi_1\phi_1'')+v_1''\phi_1'')\\
&+(-v_1^{\mathrm{IV}}(\phi_1+v_1'w_1')-w_1^{\mathrm{IV}}\phi_1^2-v_1'''(2\phi_1'+3w_1'v_1''+v_1'w_1'')-4w_1'''\phi_1\phi_1'-w_1''(2\phi'^2_1+v''^2_1+2\phi_1\phi_1'')-v_1''\phi_1'')\\
&+I_1(-\dot{v}_1'\dot{\phi}_1'-\dot{v}'^2_1 w_1''-\dot{\phi}_1\dot{v}_1''-2w_1'\dot{v}_1'\dot{v}_1'')=0, \qquad (46)
\end{aligned}
$$

- ϕ_1 direction

$$
\begin{aligned}
&D_{\xi 1}(v_1'''w_1'+v_1''w_1''+\phi_1'')+D_{\eta 1}(-\phi_1 v''^2_1+v_1''w_1''+\phi_1 w''^2_1)+(\phi_1 v''^2_1-v_1''w_1''-\phi_1 w''^2_1)\\
&\quad+I_1(-\ddot{\phi}_1-w_1'\ddot{v}_1'-\dot{v}_1'\dot{w}_1')=0, \qquad (47)
\end{aligned}
$$

- v_2 direction

$$
\begin{aligned}
&m_2(-\ddot{v}_2-\ddot{w}_{1C}\left(1-\tfrac{1}{2}\phi_{1C}^2-\tfrac{1}{2}w'^2_{1C}\right)-s_2(\ddot{\phi}_{1C}+\phi_{1C}\dot{v}'^2_{1C}-\phi_{1C}\dot{w}'^2_{1C}+\ddot{v}_{1C}'w_{1C}')-u_2(\ddot{\phi}_{1C}+\ddot{v}_{1C}'w_{1C}')\\
&+v_2(\dot{\phi}^2_{1C}+\dot{w}'^2_{1C})+w_2\ddot{w}_{1C}'-2\dot{u}_2(\dot{\phi}_{1C}+\dot{v}_{1C}'w_{1C}')+\ddot{u}_{1C}(w_{1C}'-\phi_{1C}v_{1C}')+\ddot{v}_{1C}(v_{1C}'w_{1C}'+\phi_{1C}))\\
&+\lambda_2 v_2''+D_{\xi 2}(-\phi_2'''w_2'-v_2^{IV}w'^2_2-w_2'''(\phi_2'+2w_2'v_2'')-2w_2''(2v_2'''w_2'+v_2''w_2''+\phi_2''))\\
&+D_{\eta 2}(w_2^{\mathrm{IV}}\phi_2-v_2^{\mathrm{IV}}\phi_2^2+2w_2'''\phi_2'-4v_2'''\phi_2\phi_2'-2v_2''(\phi'^2_2+\phi_2\phi_2'')+w_2''\phi_2'')\\
&+D_{\zeta 2}(-v_2^{\mathrm{IV}}(1-\phi_2^2+v_2'^2)-w_2^{\mathrm{IV}}(\phi_2+v_2'w_2')+4v_2'''(\phi_2\phi_2'-v_2'v_2'')-w_2'''(2\phi_2'+w_2'v_2''+3v_2'w_2'')\\
&+v_2''(2\phi'^2_2-v''^2_2-w''^2_2+2\phi_2\phi_2'')-w_2''\phi_2'')+I_2 m_2(\dot{w}_2'\dot{\phi}_2'+w_2'(\ddot{\phi}_2'+2\dot{w}_2'\dot{v}_2''+w_2'\ddot{v}_2''+2\dot{v}_2'\dot{w}_2'')\\
&+w_2''(\ddot{\phi}_2+2w_2'\ddot{v}_2'+2\dot{v}_2'\dot{w}_2')+\dot{\phi}_2\dot{w}_2'')=0, \qquad (48)
\end{aligned}
$$

- w_2 direction

$$
\begin{aligned}
&m_2\Big(-\ddot{w}_2+s_2\Big(\ddot{v}_{1C}'\left(1-\tfrac{1}{2}\phi_{1C}^2+\tfrac{1}{2}v'^2_{1C}\right)+\ddot{w}_{1C}'(\phi_{1C}+v_{1C}'w_{1C}')+v_{1C}'(\dot{v}'^2_{1C}+\dot{w}'^2_{1C})\Big)+u_2(\ddot{v}_{1C}'+\phi_{1C}\ddot{w}_{1C}')\\
&+v_2(\ddot{w}_{1C}'-\phi_{1C}\ddot{v}_{1C}')+w_2(\dot{v}'^2_{1C}+\dot{w}'^2_{1C})+2\dot{u}_{1C}(\dot{v}_{1C}'v_{1C}'+\dot{w}_{1C}'w_{1C}')-2\dot{v}_{1C}\dot{v}_{1C}'-2\dot{w}_{1C}\dot{w}_{1C}'\\
&-\ddot{u}_{1C}\left(1-\tfrac{1}{2}v'^2_{1C}-\tfrac{1}{2}w'^2_{1C}\right)-\ddot{v}_{1C}v_{1C}'-\ddot{w}_{1C}w_{1C}'\Big)+\lambda_2 w_2''+D_{\xi 2}(v_2'''(\phi_2'+2w_2'v_2'')+v''^2_2 w_2''+v_2''\phi_2'')\\
&+D_{\eta 2}(-w_2^{\mathrm{IV}}(1-\phi_2^2+w'^2_2)+v_2^{\mathrm{IV}}\phi_2+2v_2'''\phi_2'+4w_2'''(\phi_2\phi_2'-w_2'w_2'')+w_2''(2\phi'^2_2-w''^2_2+2\phi_2\phi_2'')+v_2''\phi_2'')\\
&+D_{\zeta 2}(-v_2^{\mathrm{IV}}(\phi_2+v_2'w_2')-w_2^{\mathrm{IV}}\phi_2^2-v_2'''(2\phi_2'+3w_2'v_2''+v_2'w_2'')-4w_2'''\phi_2\phi_2'\\
&-w_2''(2\phi'^2_2+v''^2_2+2\phi_2\phi_2'')-v_2''\phi_2'')+I_2 m_2(-\dot{v}_2'\dot{\phi}_2'-\dot{v}'^2_2 w_2''-\dot{\phi}_2\dot{v}_2''-2w_2'\dot{v}_2'\dot{v}_2'')=0, \qquad (49)
\end{aligned}
$$

- ϕ_2 direction

$$
\begin{aligned}
&D_{\xi 2}(v_2'''w_2'+v_2''w_2''+\phi_2'')+D_{\eta 2}(-\phi_2 v''^2_2+v_2''w_2''+\phi_2 w''^2_2)+D_{\zeta 2}(\phi_2 v''^2_2-v_2''w_2''-\phi_2 w''^2_2)\\
&\quad+I_2 m_2(-\ddot{\phi}_2-w_2'\ddot{v}_2'-\dot{v}_2'\dot{w}_2')=0. \qquad (50)
\end{aligned}
$$

The dimensionless boundary conditions are stated as

- at point B

$$
v_{1B}=0,\quad w_{1B}=0,\quad \phi_{1B}=0,\quad v_{1B}'=0,\quad w_{1B}'=0, \qquad (51)
$$

- at point C

$$
\begin{aligned}
&v'''_{1C} - \lambda_1 v'_{1C} - (M_2 + M_A)(\ddot{u}_{2A} + \ddot{v}_{1C}) - M_C(\ddot{v}_{1C} + g^*) - M_A g^* = 0,\\
&D_{\eta 1} w'''_{1C} - \lambda_1 w'_{1C} - (M_2 + M_A)(\ddot{v}_{2A} + \ddot{w}_{1C} + L_2\ddot{\phi}_{1C}) - M_C \ddot{w}_{1C} = 0,\\
&D_{\xi 1}\phi'_{1C} + I_{C\xi}\ddot{\phi}_{1C} + (M_2 + M_A)L_2(\ddot{v}_{2A} + \ddot{w}_{1C} + L_2\ddot{\phi}_{1C}) - M_A g^*(v_{2A} + L_2\phi_{1C}) = 0,\\
&v''_{1C} + I_{C\zeta}\ddot{v}'_{1C} - (M_2 + M_A)L_2(\ddot{w}_{2A} + \ddot{u}_{1C} - L_2\ddot{v}'_{1C}) + M_A g^*(w_{2A} - L_2 v'_{1C}) = 0,\\
&D_{\eta 1} w''_{1C} + I_{C\eta}\ddot{w}'_{1C} = 0,
\end{aligned} \tag{52}
$$

- at point A

$$
\begin{aligned}
&D_{\zeta 2} v'''_{2A} - \lambda_2 v'_{2A} - M_A(\ddot{v}_{2A} + \ddot{w}_{1C} + L_2\ddot{\phi}_{1C} + g^*\phi_{1C}) = 0,\\
&D_{\eta 2} w'''_{2A} - \lambda_2 w'_{2A} - M_A(\ddot{w}_{2A} + \ddot{u}_{1C} - L_2\ddot{v}'_{1C} + g^* v'_{1C}) = 0,\\
&D_{\xi 2}\phi'_{2A} + I_{A\xi}\ddot{\phi}_{2A} = 0,\\
&D_{\zeta 2} v''_{2A} + I_{A\zeta}\ddot{v}'_{2A} = 0,\\
&D_{\eta 2} w''_{2A} + I_{A\eta}\ddot{w}'_{2A} = 0.
\end{aligned} \tag{53}
$$

The Lagrange multipliers λ_1 and λ_2 are determined on the basis of the equations of motion and boundary conditions for the u_1 and u_2 directions, respectively,

$$
\lambda_1 = \int_1^{s_1} \ddot{u}_1\, \mathrm{d}s_1 - [(M_2 + M_A)(\ddot{w}_{2A} + \ddot{u}_{1C} - L_2\ddot{v}'_{1C}) + M_C\ddot{u}_{1C}], \tag{54}
$$

$$
\begin{aligned}
\lambda_2 = \int_{L_2}^{s_2} m_2 \Big[&\ddot{u}_2 + \ddot{v}_{1C}\left(1 - \frac{1}{2}\phi_{1C}^2 - \frac{1}{2}v'^2_{1C}\right) - s_2(\dot{\phi}_{1C}^2 + \dot{v}'^2_{1C} + 2\phi_{1C}\ddot{v}'_{1C}\dot{w}'_{1C} + 2\dot{\phi}_{1C}\dot{v}'_{1C}w'_{1C})\\
&- u_2(\dot{v}'^2_{1C} + \dot{\phi}^2_{1C}) - v_2(\ddot{\phi}_{1C} + \dot{v}'^2_{1C} + 2\dot{v}'_{1C}\dot{w}'_{1C} + \ddot{v}'_{1C}w'_{1C}) - w_2(\ddot{v}'_{1C} + \phi_{1C}\ddot{w}'_{1C})\\
&- 2\dot{v}_2(\dot{\phi}_{1C} + \dot{v}'_{1C}w'_{1C}) - \ddot{u}_{1C}(v'_{1C} + \phi_{1C}w'_{1C}) + \ddot{w}_{1C}\phi_{1C}\Big]\, \mathrm{d}s_2 - M_A(\ddot{u}_{2A} + \ddot{v}_{1C} + g^*).
\end{aligned} \tag{55}
$$

Because coordinates u_1 and u_2 are dependent on the v_1, w_1, v_2, w_2 variables, then the following equations have to be taken into account in the equations of motion given above:

$$
\begin{aligned}
u'_1 &= -\frac{1}{2}(v'^2_1 + w'^2_1), \quad u_1 = -\frac{1}{2}\int_0^{s_1}(v'^2_1 + w'^2_1)\,\mathrm{d}s_1,\\
u'_2 &= -\frac{1}{2}(v'^2_2 + w'^2_2), \quad u_2 = -\frac{1}{2}\int_0^{s_2}(v'^2_2 + w'^2_2)\,\mathrm{d}s_2.
\end{aligned}
$$

Finally we get six coupled equations of motion and 15 boundary conditions.

4. Experiment and finite element analysis

The experimental setup used for the testing work is composed of a high-end proprietary modal analysis system, spectral acquisition software, and an electrically matched shaker with control of the excitation level. The signals are measured by three small, low mass, piezo-sensors and a piezo-sensor is used for monitoring the excitation. The arrows in Fig. 1 indicate the orientations of the sensors used in the experimental tests.

Preliminary experimental investigations consisted of tuning the structure for chosen bending and torsional natural frequencies of the structure. The frequencies are determined by modal analysis of the system response activated by an impact. By modification of lumped masses A and C and the length of the primary beam, the system has been tuned for a 1:4 ratio of the first bending frequency of the primary beam ($\omega_{b1(\mathrm{I})} = 3.61$ Hz) and the first bending frequency of the secondary beam ($\omega_{b1(\mathrm{II})} = 14.45$ Hz). The torsional frequency of the primary beam, when the whole structure is fixed, has also been measured ($\omega_{t1(\mathrm{I})} = \sim 4.9$ Hz). The parameters of the tuned structure are listed in Table 1. After the tuning procedure, the whole structure is mounted on the shaker and then excited by a random excitation over the band from 0 to 40 Hz. This test enables the main resonant responses of the system to be found. Figs. 3 and 4 show, respectively, the frequency spectra of the system responses obtained from sensors no. 1 (Z direction) and no. 3 (Y direction). The highest peaks in Fig. 3 correspond to the resonant frequencies of the system, which in a linear system are equal to the natural frequencies. Individual peaks, in turn, correspond to the first bending frequency $\omega_{b1(\mathrm{I})} = 3.61\,\mathrm{Hz}$, the first torsional frequency $\omega_{t1(\mathrm{I})} = 4.9\,\mathrm{Hz}$, and the second free bending frequency $\omega_{b2(\mathrm{I})} = 15.50\,\mathrm{Hz}$, of the primary beam. Because of the positioning of the sensor no. 3, Fig. 4 mainly shows the dynamics of the primary beam. The closeness of the torsion and bending frequencies is a typical feature of such a structure when made of composite material. For geometrically equivalent aluminium or steel beams, the torsion natural frequency would tend to be remote from the bending frequencies.

The structure has been also modelled in the ABAQUS$^{\mathrm{TM}}$ commercial finite element code for natural frequencies and mode shape extraction. The composite beams are modelled by fully integrated shell elements S4 with 6 degrees of freedom per node and a consistent mass matrix. The elements are based on Mindlin–Reissner theory with finite membrane strain. The material is a layered composite material with proper orientation of each orthotropic layer, and with three integration points through the thickness.

Table 1
Parameters for structure after tuning 1:4

Length of horizontal beam	236 mm
Length of vertical beam	201 mm
Mass A value	15.3 g
Mass C value	38.0 g

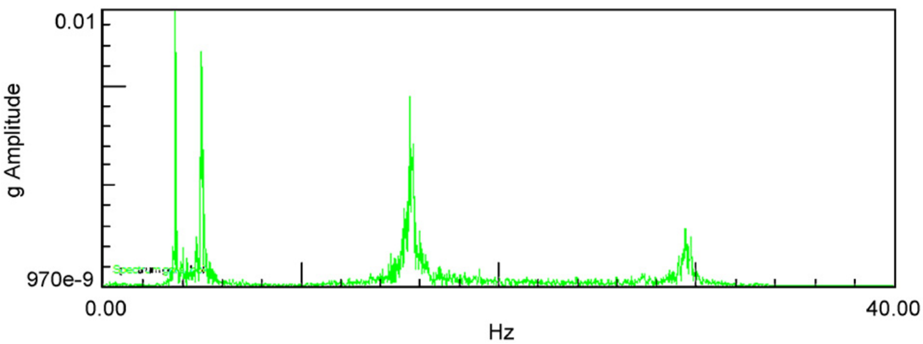

Fig. 3. Spectrum of the response measured by sensor no. 1.

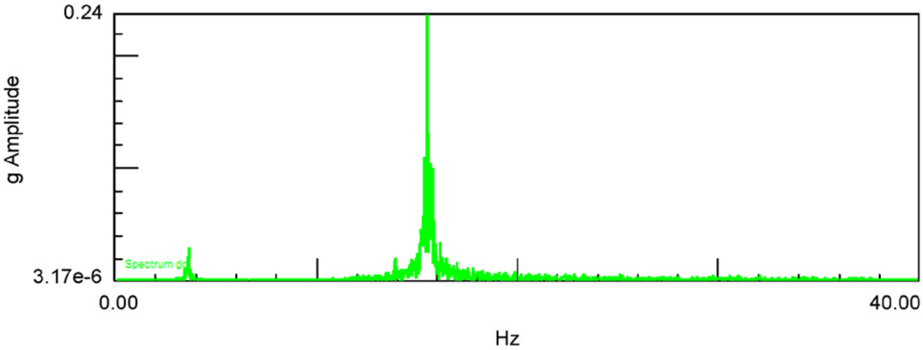

Fig. 4. Spectrum of the response measured by sensor no. 3.

The natural frequency and mode extraction procedure was applied after one geometrically nonlinear step of gravity loading of the flexible L-beam structure. In this way, the reference state of the structure accounts for the large displacements and rotations leading to its deformed shape and the stiffness matrix used in the analysis is the tangential stiffness of the deformed structure. The nonlinear preloading gives up to 2.5% difference in the natural frequencies from the case of the unloaded structure.

The results based on the modal analysis of the finite element method (FEM) model and those obtained experimentally are compared in Table 2. Vibration modes which correspond to the frequencies presented in Table 2 are shown in Fig. 5. For better visualisation the modes of vibrations are plotted together with the undeformed model. The first mode with the lowest frequency value, that is 3.61 Hz (the first peak in Figs. 3 and 4) is given in Fig. 5(a), evidently the first bending mode of the primary beam is responsible for the dynamics. The vertical beam moves in the vertical plane as a solid body. The mode at 4.9 Hz represents torsion of the primary beam (Fig. 5(b), the second peak in Fig. 3) while the mode at 15.5 Hz corresponds to the second bending mode of the primary beam (Fig. 5(c) and the third peak in Figs. 3 and 4). It is worth noting that the three lowest vibration modes, which have been separated by linear modal analysis, only exhibit deformations in bending and torsion of the primary beam. The secondary beam, which has the same cross-section, remains undeformed.

Table 2
Comparison—experiment and FEM results

	Physical model (Hz)	FEM model (Hz)
Fig. 5(a)	3.61	3.78
Fig. 5(b)	4.90	4.21
Fig. 5(c)	15.50	16.10
Fig. 5(d)	29.60	29.25

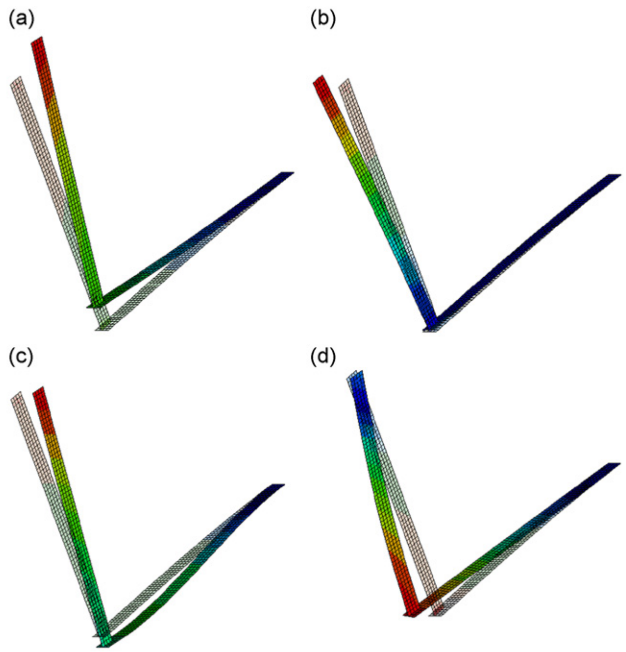

Fig. 5. Vibration modes of the structure: (a) the first bending mode of the primary beam; (b) the first torsional mode of the primary beam; (c) the second bending mode of the primary beam; and (d) the first bending mode of the primary beam in the stiffer direction coupled with bending mode of the secondary beam.

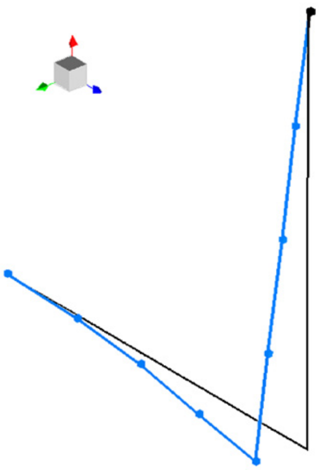

Fig. 6. Experimental modal analysis, equivalent to Fig. 5(d).

An interesting phenomenon has been observed by studying the fourth peak of Fig. 3 in detail. For this frequency the bending mode of the vertical beam is excited, and, due to interaction, the bending mode of the horizontal beam in the stiff direction is excited too. Point C moves in the horizontal plane while the node of vibration is localised very close to point A (top mass). This out-of-plane motion is presented in Fig. 5(d) and it is confirmed experimentally in Fig. 6. This (the fourth) mode of vibrations is the object of further analysis. The authors have not found this kind of behaviour to be evident in ''L''-shaped structures before, nor does there appear to be evidence of discussions of such phenomena in the literature. As evident in Table 2 experimental and FEA results for this mode are in a very good agreement. The next paragraph presents preliminary numerical investigations of this mode.

In many practical engineering applications, the control of the motion of the top mass A plays an important role. Therefore, the influence of the internal resonance conditions on trajectories at this point is of interest. By imposing harmonic excitations at different frequencies, in particular around the resonant areas, the response of the system can be investigated in some detail. As mentioned earlier, the two first frequencies, torsional and flexural, of the composite structure are very close localised. Therefore, behaviour of the system for excitations close to the first torsional frequency of the primary beam, is studied experimentally, as well. To avoid damage to the structure, and to get satisfactory signals, the amplitude of excitation has been carefully chosen. Fig. 7 shows trajectories of the top mass near the torsional resonance of the primary beam. The trajectories are reconstructed by signals received from sensors no. 1 and 2. During transition through the resonance, differences in the structural response are clearly visible. Inside the resonance area, near 4.9 Hz, the major axis of an elliptic trajectory is almost parallel to the Z coordinate. Outside this resonance zone the axis rotates in the clockwise direction and the trajectory, because of nonlinear interactions with other vibration modes, assumes a more complex shape, reminiscent of a Lissajous figure.

5. Analysis of the out-of-plane response

To study the dynamical response of the system, the set of partial differential equations has been discretised by applying the Galerkin method. Solutions of the system are assumed to be in the form

$$v_1 = \sum_{i=1}^{n} a_{vi}(\tau)\alpha_{vi}(s_1), \quad w_1 = \sum_{i=1}^{n} a_{wi}(\tau)\alpha_{wi}(s_1), \quad \phi_1 = \sum_{i=1}^{n} a_{\phi i}(\tau)\alpha_{\phi i}(s_1),$$
$$v_2 = \sum_{i=1}^{n} b_{vi}(\tau)\beta_{vi}(s_2), \quad w_2 = \sum_{i=1}^{n} b_{wi}(\tau)\beta_{wi}(s_2), \quad \phi_2 = \sum_{i=1}^{n} b_{\phi i}(\tau)\beta_{\phi i}(s_2), \tag{56}$$

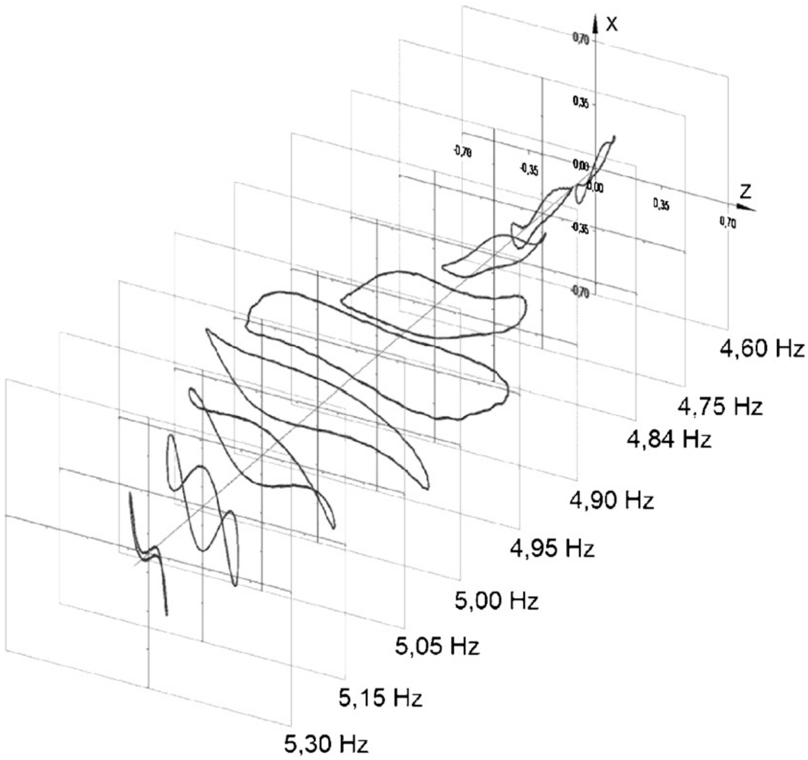

Fig. 7. Trajectories of the top mass.

where $a_{vi}(\tau)$, $a_{wi}(\tau)$, $a_{\phi i}(\tau)$, $b_{vi}(\tau)$, $b_{wi}(\tau)$, $b_{\phi i}(\tau)$ are time dependent and are the so-called Galerkin coefficients. $\alpha_{vi}(s_1)$, $\alpha_{wi}(s_1)$, $\alpha_{\phi i}(s_1)$, $\beta_{vi}(s_2)$, $\beta_{wi}(s_2)$, $\beta_{\phi i}(s_2)$ are corresponding mode shapes, and n is the number of assumed modes. Note that the notation $a(\tau)$ and $\alpha(s_1)$ corresponds to the primary beam, and $b(\tau)$, $\beta(s_2)$ to the secondary beam.

Substituting Eq. (56) into the partial differential Eqs. (45)–(50) and assuming only one mode response for each coordinate ($n = 1$), we get

$$\ddot{a}_v + k_{av}a_v = -\varepsilon(\kappa_{aw,a\phi}a_w a_\phi + \mu_{\dot{a}w,\dot{a}\phi}\dot{a}_w\dot{a}_\phi + \mu_{av,\ddot{a}v}a_v\ddot{a}_v + \mu_{aw,\ddot{a}\phi}a_w\ddot{a}_\phi + \mu_{av,\ddot{b}w}a_v\ddot{b}_w) + \varepsilon^2(\ldots),$$

$$\ddot{a}_w + k_{aw}a_w = -\varepsilon(\kappa_{av,a\phi}a_v a_\phi + \mu_{\dot{a}v,\dot{a}\phi}\dot{a}_v\dot{a}_\phi + \mu_{aw,\ddot{a}v(2)}a_w\ddot{a}_v + \mu_{aw,\ddot{b}w}a_w\ddot{b}_w) + \varepsilon^2(\ldots),$$

$$\ddot{a}_\phi + k_{a\phi}a_\phi = -\varepsilon(\kappa_{av,aw}a_v a_w + \mu_{\dot{a}v,\dot{a}w}\dot{a}_v\dot{a}_w + \mu_{aw,\ddot{a}v(3)}a_w\ddot{a}_v) + \varepsilon^2(\ldots),$$

$$\begin{aligned}\ddot{b}_v + k_{bv}b_v = &-\varepsilon(\mu_{\ddot{a}w}\ddot{a}_w + \mu_{\ddot{a}\phi}\ddot{a}_\phi + \kappa_{bw,b\phi}b_w b_\phi + \mu_{\dot{b}w,\dot{b}\phi}\dot{b}_w\dot{b}_\phi + \mu_{aw,\ddot{a}v}a_w\ddot{a}_v \\ &+ \mu_{a\phi,\ddot{a}v}a_\phi\ddot{a}_v + \mu_{bv,\ddot{a}v}b_v\ddot{a}_v + \mu_{bw,\ddot{a}w}b_w\ddot{a}_w + \mu_{bw,\ddot{b}\phi}b_w\ddot{b}_\phi) + \varepsilon^2(\ldots),\end{aligned}$$

$$\begin{aligned}\ddot{b}_w + k_{bw}b_w = &-\varepsilon(\mu_{\ddot{a}v}\ddot{a}_v + \kappa_{bv,b\phi}b_v b_\phi + \mu_{\dot{a}v,\dot{a}v}\dot{a}_v^2 + \mu_{\dot{a}w,\dot{a}w}\dot{a}_w^2 + \mu_{\dot{b}v,\dot{b}\phi}\dot{b}_v\dot{b}_\phi + \mu_{av,\ddot{a}v}a_v\ddot{a}_v \\ &+ \mu_{bw,\ddot{a}v}b_w\ddot{a}_v + \mu_{aw,\ddot{a}w}a_w\ddot{a}_w + \mu_{a\phi,\ddot{a}w}a_\phi\ddot{a}_w + \mu_{bv,\ddot{a}w}b_v\ddot{a}_w) + \varepsilon^2(\ldots),\end{aligned}$$

$$\ddot{b}_\phi + k_{b\phi}b_\phi = -\varepsilon(\kappa_{bv,bw}b_v b_w + \mu_{\dot{b}v,\dot{b}w}\dot{b}_v\dot{b}_w + \mu_{bw,\ddot{b}v}b_w\ddot{b}_v) + \varepsilon^2(\ldots). \quad (57)$$

In this paper, the analytical approach is concentrated only on the out-of-plane motion, represented by the fourth mode response, obtained by FEA (Fig. 5(d)), and confirmed by real experimental tests (Fig. 6).

However, the proposed Galerkin approach initially needs to be used to solve the nonlinear boundary condition problem, and that can cause difficulty. Therefore, the mode shapes are determined on the basis of FEM. Analysing in detail the deformations of the structure presented in Fig. 5(d) as obtained by FE method, it can be concluded that the total deformation can be composed of the individual modes of each beam, taking into account their torsional and flexural deformation components. The out-of-plane motion consists of the first shape modes for the w_1, ϕ_1, v_2, w_2, ϕ_2 coordinates and the third mode for the v_1 coordinate. The mode shapes presented in Fig. 8 are equivalent to those modes obtained from FEM. The shape functions presented in Fig. 8 can be assumed to be in the classical form, e.g. in the v_1 direction

$$\alpha_v = C_{\alpha v1}\cosh(\lambda s_1) + C_{\alpha v2}\sinh(\lambda s_1) + C_{\alpha v3}\cos(\lambda s_1) + C_{\alpha v4}\sin(\lambda s_1), \tag{58}$$

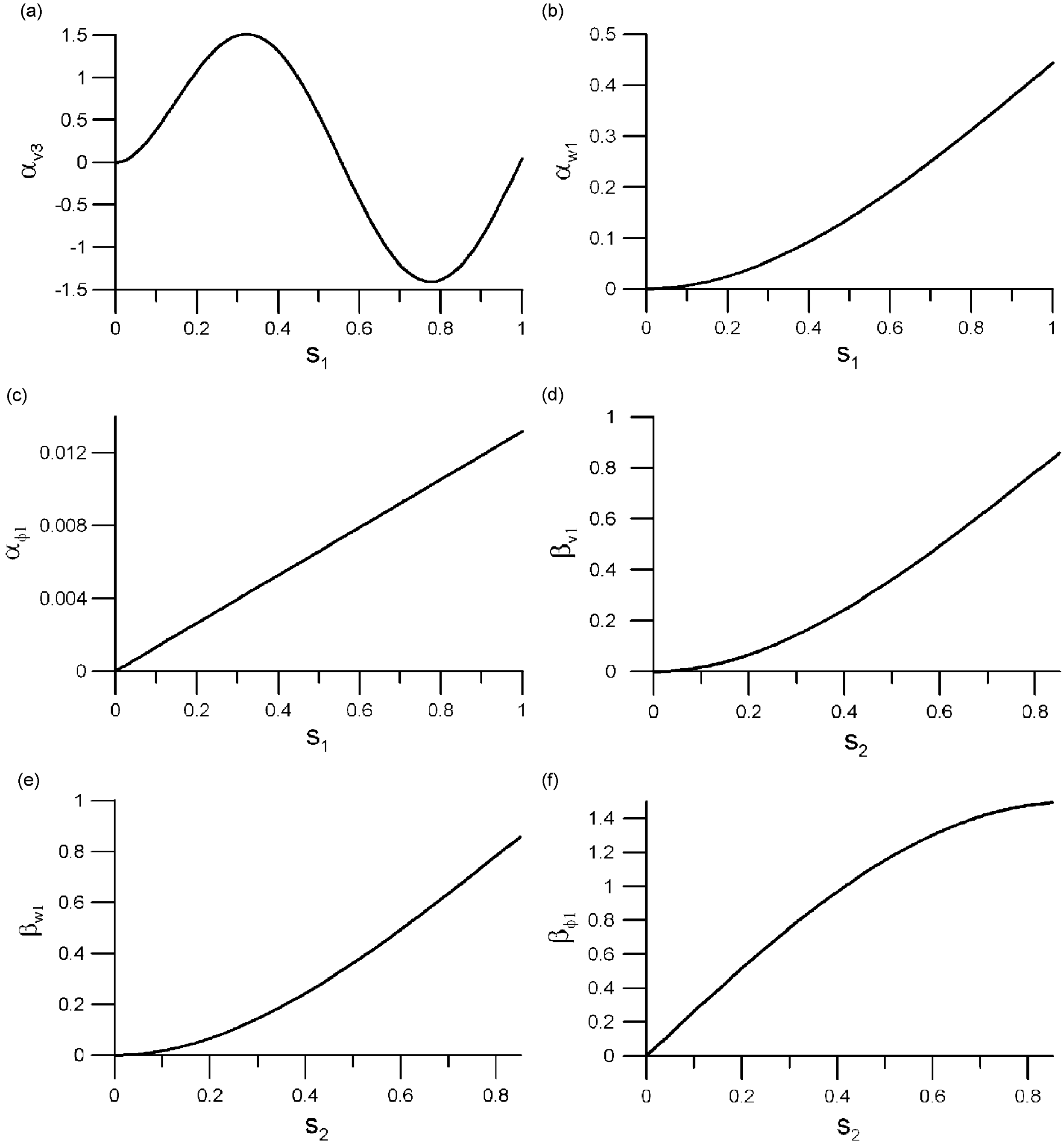

Fig. 8. Shape functions of the out-of-plane resonance: (a) beam 1—bending in flexible direction; (b) beam 1—bending in stiff direction; (c) beam 1—torsion; (d) beam 2—bending in flexible direction; (e) beam 2—bending in stiff direction; and (f) beam 2—torsion.

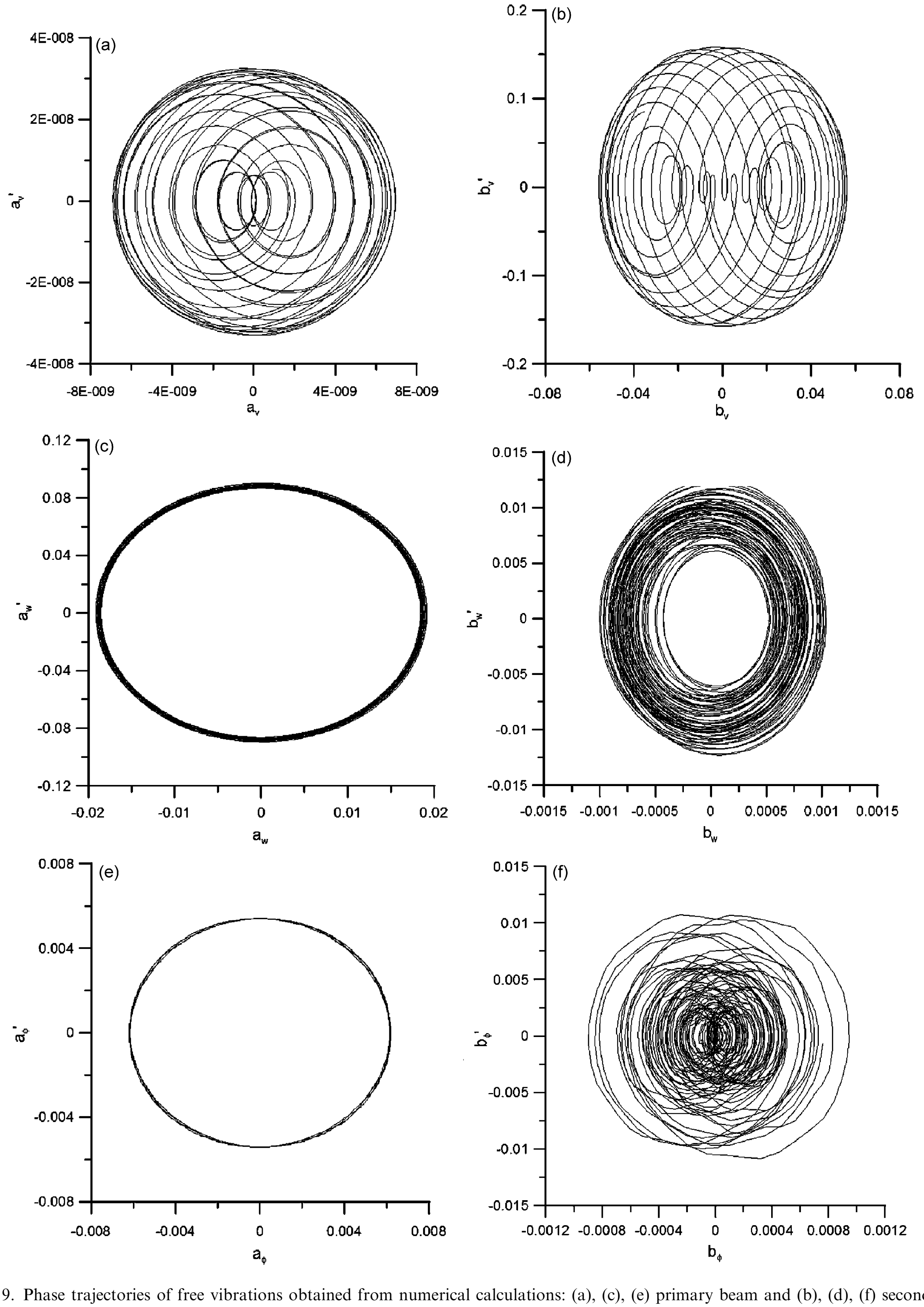

Fig. 9. Phase trajectories of free vibrations obtained from numerical calculations: (a), (c), (e) primary beam and (b), (d), (f) secondary beam.

while the orthogonality property of the assumed mode is defined by taking the attached lumped masses at point C and A, and takes following form:

$$\alpha_{vi}(x)\alpha_{vj}(x)\,\mathrm{d}x + m\alpha_{vi}(l)\alpha_{vj}(l) = \begin{cases} 1 & \text{for } i=j, \\ 0 & \text{for } i \neq j, \end{cases} \tag{59}$$

where for the primary beam: $m = m_2 + M_A + M_C$ for the α_v and α_w modes, and $m = (I_{C\xi} + M_2L_2^2 + M_AL_2^2)/I_1$ for the α_ϕ mode, and for the secondary beam $m = M_A/m_2$ for the β_v and β_w modes and $m = I_{A\xi}/(m_2I_2)$ for the β_ϕ mode.

To simplify the integration procedure using the Mathematica® package, Eq. (58) have been approximated by polynomials

$$\alpha_v^* = B_{\alpha v2}s_1^2 + B_{\alpha v3}s_1^3 + \cdots + B_{\alpha v10}s_1^{10}. \tag{60}$$

Definitions of the coefficients included in Eqs. (57) are presented in Appendix A.

Physical data of the composite material such as Young's modulus, Poisson's ratio, density of the material, etc., have been determined on the basis of several experimental tests. Physical data of the structure and the coefficients of Eqs. (57) are included in Appendix A. From there a numerical model in the Matlab-Simulink package could be created. The excitation has been included by adding the term $v_{10}\vartheta^2 \cos \vartheta\tau$ on the right-hand side in the first equation. Small modal damping (0.1%) has been added to all coordinates of the system, as well. Phase trajectories obtained from the numerical calculations are presented in Fig. 9, where axes represent displacement and the first time derivative, respectively. As can be seen, the behaviour of the system, especially for coordinates v_1 and v_2, is very complicated. Comparison of the frequencies of the system response obtained

Table 3
Comparison—experiment and numerical model

	Physical model (Hz)	Numerical model (Hz)
Fig. 5(b)	4.90	5.69
Fig. 5(d)	29.60	28.45

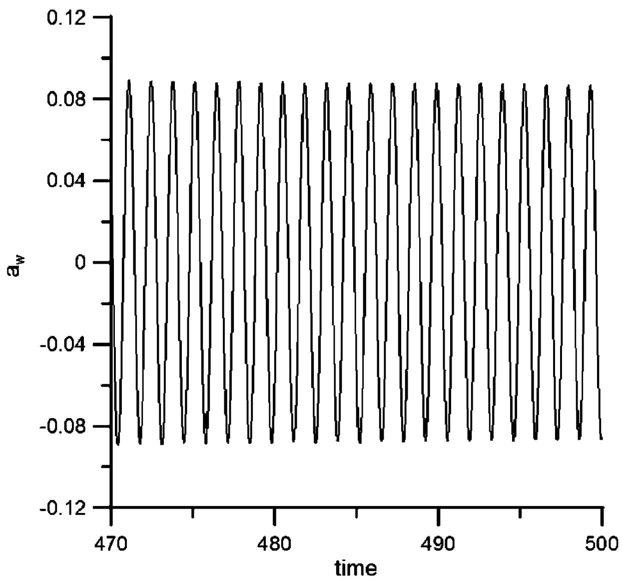

Fig. 10. Time series of displacement for free vibrations—w_1 direction.

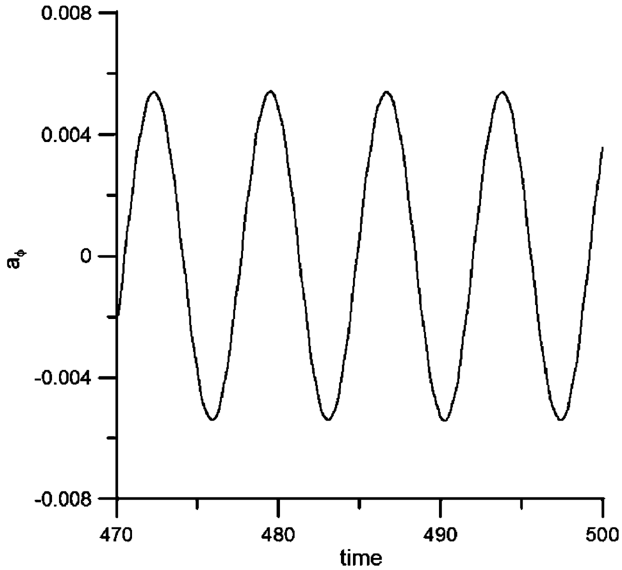

Fig. 11. Time series of displacement for free vibrations—ϕ_1 direction.

from the numerical model and the physical system is presented in Table 3. Numerical frequencies are obtained directly from time histories received from the Simulink software (Figs. 10 and 11) and next by converting them to dimensional form. The analytical results obtained for the fourth mode of vibration (Fig. 5(d)) are very close to those obtained by experiment. Identification of the system parameters, especially estimation of the damping coefficients, and fitting the numerical model with the real system will be the next step of the work.

6. Conclusions and final remarks

The paper deals with preliminary theoretical and well-developed experimental studies of an autoparametric beam structure with essentially different stiffnesses in two orthogonal directions. The systematically derived equations of motion, and a preliminary series of numerical calculations, show that nonlinear terms which couple the structure may result in many unexpected responses. An experimentally tested composite beam structure, tuned for the 1:4 internal resonance condition, exhibits possible vibrations as an out-of-plane motion in the stiff direction of the primary beam. In the neighbourhood of the torsional resonance, due to nonlinear coupling, additional nonlinear modes are involved in the system response, and this is expressed by the complex trajectories that have been seen. The experimental work has confirmed the FEA analysis, with generally very good agreement. Therefore the results give a promising basis for finding and interpreting analytical solutions of the mathematical model. This, and further investigation will eventually allow a strategy to be developed for the active control of this kind of structure by the application of PZT or SMA elements.

Acknowledgments

The work is supported by Grants N502 049 31/1449 and 65/6.PR UE/2005/7 of the Polish Ministry of Science and Higher Education. The authors wish to express their gratitude to Marie Curie Transfer of Knowledge programme for the support of project MKTD-CT-2004-014058, which gave the opportunity for their cooperation.

Appendix A

A.1. Physical parameters of the structure

$$E_1 = E_2 = 25.5\,\text{GPa}, \quad I_{A\xi} = 7.821 \times 10^{-9}\,\text{kg}\,\text{m}^2,$$
$$G_1 = G_2 = 9.8\,\text{GPa}, \quad I_{A\eta} = 12.889 \times 10^{-9}\,\text{kg}\,\text{m}^2,$$
$$\rho_1 = \rho_2 = 2100\,\text{kg}\,\text{m}^{-3}, \quad I_{A\zeta} = 5.2476 \times 10^{-9}\,\text{kg}\,\text{m}^2,$$
$$a_1 = a_2 = 2.1\,\text{mm}, \quad I_{C\xi} = 111.6 \times 10^{-9}\,\text{kg}\,\text{m}^2,$$
$$b_1 = b_2 = 12.8\,\text{mm}, \quad I_{C\eta} = 75.7 \times 10^{-9}\,\text{kg}\,\text{m}^2,$$
$$l_1 = 236\,\text{mm}, \quad I_{C\zeta} = 156.6 \times 10^{-9}\,\text{kg}\,\text{m}^2,$$
$$l_2 = 201\,\text{mm}, \quad \beta_1 = \beta_2 = 0.3,$$
$$m_A = 0.0153\,\text{kg},$$
$$m_C = 0.038\,\text{kg},$$

$$D_{\xi 1} = G_1 J_{\xi 1}, \quad J_{\xi 1} = \beta_1 b_1 a_1^3, \quad D_{\xi 2} = G_1 J_{\xi 2}, \quad J_{\xi 2} = \beta_2 b_2 a_2^3,$$
$$D_{\eta 1} = E_1 J_{\eta 1}, \quad J_{\eta 1} = \frac{a_1 b_1^3}{12}, \quad D_{\eta 2} = E_1 J_{\eta 2}, \quad J_{\eta 2} = \frac{a_2 b_2^3}{12},$$
$$D_{\zeta 1} = E_1 J_{\zeta 1}, \quad J_{\zeta 1} = \frac{b_1 a_1^3}{12}, \quad D_{\zeta 2} = E_1 J_{\zeta 2}, \quad J_{\zeta 2} = \frac{b_2 a_2^3}{12}.$$
$$A_1 = a_1 b_1, \quad A_2 = a_2 b_2,$$

A.2. Definition of the coefficients of Eq. (57)

- primary beam

$$k_{av} = \frac{\int_0^1 D_{\zeta 1} \alpha_v^{\text{IV}} \alpha_v \, \text{d}s_1}{\int_0^1 \alpha_v^2 \, \text{d}s_1},$$

$$\kappa_{aw,a\phi} = -\frac{\int_0^1 ((D_{\eta 1} - D_{\zeta 1})(\alpha_w^{\text{IV}} \alpha_\phi + 2\alpha_w''' \alpha_\phi' + \alpha_w'' \alpha_\phi'') - D_{\xi 1}(\alpha_\phi''' \alpha_w' + \alpha_w''' \alpha_\phi' + 2\alpha_w'' \alpha_\phi''))\alpha_v \, \text{d}s_1}{\int_0^1 \alpha_v^2 \, \text{d}s_1},$$

$$\mu_{\dot{a}w,\dot{a}\phi} = -\frac{\int_0^1 I_1(\alpha_w' \alpha_\phi' + \alpha_w'' \alpha_\phi)\alpha_v \, \text{d}s_1}{\int_0^1 \alpha_v^2 \, \text{d}s_1}, \quad \mu_{av,\ddot{a}v} = -\frac{\int_0^1 (M_2 + M_A) L_2 \alpha_v'' \alpha_{vC}' \alpha_v \, \text{d}s_1}{\int_0^1 \alpha_v^2 \, \text{d}s_1},$$

$$\mu_{aw,\ddot{a}\phi} = -\frac{\int_0^1 I_1(\alpha_w' \alpha_\phi' + \alpha_w'' \alpha_\phi)\alpha_v \, \text{d}s_1}{\int_0^1 \alpha_v^2 \, \text{d}s_1}, \quad \mu_{av,\ddot{b}w} = \frac{\int_0^1 (M_2 + M_A) \beta_{wA} \alpha_v'' \alpha_v \, \text{d}s_1}{\int_0^1 \alpha_v^2 \, \text{d}s_1},$$

$$k_{aw} = \frac{\int_0^1 D_{\eta 1} \alpha_w^{IV} \alpha_w \, \text{d}s_1}{\int_0^1 \alpha_w^2 \, \text{d}s_1},$$

$$\kappa_{av,a\phi} = -\frac{\int_0^1 (D_{\xi 1}(\alpha_v'''\alpha_\phi' + \alpha_v''\alpha_\phi'') + (D_{\eta 1} - D_{\zeta 1})(\alpha_v^{\mathrm{IV}}\alpha_\phi + 2\alpha_v'''\alpha_\phi' + \alpha_v''\alpha_\phi''))\alpha_w \, \mathrm{d}s_1}{\int_0^1 \alpha_w^2 \, \mathrm{d}s_1},$$

$$\mu_{\dot{a}v,\dot{a}\phi} = \frac{\int_0^1 I_1(\alpha_v'\alpha_\phi' + \alpha_\phi\alpha_v'')\alpha_w \, \mathrm{d}s_1}{\int_0^1 \alpha_w^2 \, \mathrm{d}s_1}, \quad \mu_{aw,\ddot{a}v(2)} = -\frac{\int_0^1 (M_2 + M_A)L_2\alpha_w''\alpha_{vC}'\alpha_w \, \mathrm{d}s_1}{\int_0^1 \alpha_w^2 \, \mathrm{d}s_1},$$

$$\mu_{aw,\ddot{b}w} = \frac{\int_0^1 (M_2 + M_A)\beta_{wA}\alpha_w''\alpha_w \, \mathrm{d}s_1}{\int_0^1 \alpha_w^2 \, \mathrm{d}s_1}, \quad k_{a\phi} = -\frac{\int_0^1 D_{\xi 1}\alpha_\phi''\alpha_\phi \, \mathrm{d}s_1}{\int_0^1 I_1\alpha_\phi^2 \, \mathrm{d}s_1},$$

$$\kappa_{av,aw} = -\frac{\int_0^1 (D_{\xi 1}\alpha_v'''\alpha_w' + (D_{\xi 1} + D_{\eta 1} - D_{\zeta 1})\alpha_v''\alpha_w'')\alpha_\phi \, \mathrm{d}s_1}{\int_0^1 I_1\alpha_\phi^2 \, \mathrm{d}s_1}, \quad \mu_{\dot{a}v,\dot{a}w} = \frac{\int_0^1 \alpha_v'\alpha_w'\alpha_\phi \, \mathrm{d}s_1}{\int_0^1 \alpha_\phi^2 \, \mathrm{d}s_1},$$

$$\mu_{aw,\ddot{a}v(3)} = \frac{\int_0^1 \alpha_v'\alpha_w'\alpha_\phi \, \mathrm{d}s_1}{\int_0^1 \alpha_\phi^2 \, \mathrm{d}s_1}.$$

- secondary beam

$$k_{bv} = \frac{\int_0^{L_2} (D_{\zeta 2}\beta_v^{\mathrm{IV}} + M_A g^* \beta_v'')\beta_v \, \mathrm{d}s_2}{\int_0^{L_2} m_2\beta_v^2 \, \mathrm{d}s_2}, \quad \mu_{\ddot{a}w} = \frac{\int_0^{L_2} \alpha_{wC}\beta_v \, \mathrm{d}s_2}{\int_0^{L_2} \beta_v^2 \, \mathrm{d}s_2}, \quad \mu_{\ddot{a}\phi} = \frac{\int_0^{L_2} s_2\alpha_{\phi C}\beta_v \, \mathrm{d}s_2}{\int_0^{L_2} \beta_v^2 \, \mathrm{d}s_2},$$

$$\kappa_{bw,b\phi} = -\frac{\int_0^{L_2} ((D_{\eta 2} - D_{\zeta 2})(\beta_w^{\mathrm{IV}}\beta_\phi + 2\beta_w'''\beta_\phi' + \beta_w''\beta_\phi'') - D_{\xi 2}(\beta_w'\beta_\phi''' + 2\beta_w''\beta_\phi'' + \beta_w'''\beta_\phi'))\beta_v \, \mathrm{d}s_2}{\int_0^{L_2} m_2\beta_v^2 \, \mathrm{d}s_2},$$

$$\mu_{\dot{b}w,\dot{b}\phi} = -\frac{\int_0^{L_2} I_2(\beta_w'\beta_\phi' + \beta_\phi\beta_w'')\beta_v \, \mathrm{d}s_2}{\int_0^{L_2} \beta_v^2 \, \mathrm{d}s_2}, \quad \mu_{aw,\ddot{a}v} = \frac{\int_0^{L_2} s_2\alpha_{vC}'\alpha_{wC}'\beta_v \, \mathrm{d}s_2}{\int_0^{L_2} \beta_v^2 \, \mathrm{d}s_2}, \quad \mu_{a\phi,\ddot{a}v} = -\frac{\int_0^{L_2} \alpha_{vC}\alpha_{\phi C}\beta_v \, \mathrm{d}s_2}{\int_0^{L_2} \beta_v^2 \, \mathrm{d}s_2},$$

$$\mu_{bv,\ddot{a}v} = -\frac{\int_0^{L_2} \left(m_2\beta_v'' \int_{L_2}^{s_2} \alpha_{vC} \, \mathrm{d}s_2 - M_A\alpha_{vC}\beta_v''\right)\beta_v \, \mathrm{d}s_2}{\int_0^{L_2} m_2\beta_v^2 \, \mathrm{d}s_2}, \quad \mu_{bw,\ddot{a}w} = -\frac{\int_0^{L_2} \alpha_{wC}'\beta_w\beta_v \, \mathrm{d}s_2}{\int_0^{L_2} \beta_v^2 \, \mathrm{d}s_2},$$

$$\mu_{bw,\ddot{b}\phi} = -\frac{\int_0^{L_2} I_2(\beta_w'\beta_\phi' + \beta_w''\beta_\phi)\beta_v \, \mathrm{d}s_2}{\int_0^{L_2} \beta_v^2 \, \mathrm{d}s_2}, \quad k_{bw} = \frac{\int_0^{L_2} (D_{\eta 2}\beta_w^{IV} + M_A g^* \beta_w'')\beta_w \, \mathrm{d}s_2}{\int_0^{L_2} m_2\beta_w^2 \, \mathrm{d}s_2},$$

$$\mu_{\ddot{a}v} = -\frac{\int_0^{L_2} s_2\alpha_{vC}'\beta_w \, \mathrm{d}s_2}{\int_0^{L_2} \beta_w^2 \, \mathrm{d}s_2},$$

$$\kappa_{bv,b\phi} = -\frac{\int_0^{L_2} ((D_{\eta 2} - D_{\zeta 2})(\beta_v^{\mathrm{IV}}\beta_\phi + 2\beta_v'''\beta_\phi' + \beta_v''\beta_\phi'') + D_{\xi 2}(\beta_v'''\beta_\phi' + \beta_v''\beta_\phi''))\beta_w \, \mathrm{d}s_2}{\int_0^{L_2} m_2\beta_w^2 \, \mathrm{d}s_2},$$

$$\mu_{\dot{a}v,\dot{a}v} = -\frac{\int_0^{L_2}(\alpha'^2_{vC} - 2\alpha_{vC}\alpha'_{vC})\beta_w\,\mathrm{d}s_2}{\int_0^{L_2}\beta_w^2\,\mathrm{d}s_2}, \quad \mu_{\dot{a}w,\dot{a}w} = -\frac{\int_0^{L_2}(\alpha'^2_{wC} - 2\alpha_{wC}\alpha'_{wC})\beta_w\,\mathrm{d}s_2}{\int_0^{L_2}\beta_w^2\,\mathrm{d}s_2},$$

$$\mu_{\dot{b}v,\dot{b}\phi} = \frac{\int_0^{L_2} I_2(\beta'_v\beta'_\phi + \beta_\phi\beta''_v)\beta_w\,\mathrm{d}s_2}{\int_0^{L_2}\beta_w^2\,\mathrm{d}s_2}, \quad \mu_{av,\ddot{a}v} = -\frac{\int_0^{L_2}(\alpha'^2_{vC} - \alpha_{vC}\alpha'_{vC})\beta_w\,\mathrm{d}s_2}{\int_0^{L_2}\beta_w^2\,\mathrm{d}s_2},$$

$$\mu_{bw,\ddot{a}v} = -\frac{\int_0^{L_2}\left(m_2\beta''_w\int_{L_2}^{s_2}\alpha_{vC}\,\mathrm{d}s_2 - M_A\alpha_{vC}\beta''_w\right)\beta_w\,\mathrm{d}s_2}{\int_0^{L_2} m_2\beta_w^2\,\mathrm{d}s_2}, \quad \mu_{aw,\ddot{a}w} = -\frac{\int_0^{L_2}(\alpha'^2_{wC} - \alpha_{wC}\alpha'_{wC})\beta_w\,\mathrm{d}s_2}{\int_0^{L_2}\beta_w^2\,\mathrm{d}s_2},$$

$$\mu_{a\phi,\ddot{a}w} = -\frac{\int_0^{L_2} s_2\alpha'_{wC}\alpha_{\phi C}\beta_w\,\mathrm{d}s_2}{\int_0^{L_2}\beta_w^2\,\mathrm{d}s_2}, \quad \mu_{bv,\ddot{a}w} = -\frac{\int_0^{L_2}\alpha'_{wC}\beta_v\beta_w\,\mathrm{d}s_2}{\int_0^{L_2}\beta_w^2\,\mathrm{d}s_2}, \quad k_{b\phi} = -\frac{\int_0^{L_2} D_{\xi 2}\beta''_\phi\beta_\phi\,\mathrm{d}s_2}{\int_0^{L_2} I_2 m_2\beta_\phi^2\,\mathrm{d}s_2},$$

$$\kappa_{bv,bw} = -\frac{\int_0^{L_2}(D_{\xi 2}\beta'''_v\beta'_w + (D_{\xi 2} + D_{\eta 2} - D_{\zeta 2})\beta''_v\beta''_w)\beta_\phi\,\mathrm{d}s_2}{\int_0^{L_2} I_2 m_2\beta_\phi^2\,\mathrm{d}s_2}, \quad \mu_{\dot{b}v,\dot{b}w} = \frac{\int_0^{L_2}\beta'_v\beta'_w\beta_\phi\,\mathrm{d}s_2}{\int_0^{L_2}\beta_\phi^2\,\mathrm{d}s_2},$$

$$\mu_{bw,\ddot{b}v} = \frac{\int_0^{L_2}\beta'_v\beta'_w\beta_\phi\,\mathrm{d}s_2}{\int_0^{L_2}\beta_\phi^2\,\mathrm{d}s_2}.$$

A.3. Values of the coefficients

- primary beam

$k_{av} = 2523.52$,	$\kappa_{av,aw} = 1.7575 \times 10^7$,	$\mu_{\dot{a}v,\dot{a}w} = 14.7653$,
$k_{aw} = 21.9026$,	$\kappa_{av,a\phi} = 2408.99$,	$\mu_{\dot{a}v,\dot{a}\phi} = 0.000315835$,
$k_{a\phi} = 0.953403$,	$\kappa_{aw,a\phi} = 0.149711$,	$\mu_{\dot{a}w,\dot{a}\phi} = 1.27007 \times 10^{-7}$,
$\mu_{av,\ddot{a}v} = 745.872$,	$\mu_{aw,\ddot{a}v(2)} = -21.6252$,	$\mu_{aw,\ddot{a}v(3)} = 14.7653$,
$\mu_{aw,\ddot{a}\phi} = 1.27007 \times 10^{-7}$,	$\mu_{av,\ddot{b}w} = -74.4068$,	$\mu_{aw,\ddot{b}w} = 2.15729$.

A.4. Values of the coefficients

- secondary beam

$k_{bv} = 3.65204$,	$\kappa_{bv,bw} = -272942$,	$\mu_{\ddot{a}v} = -11.6524$,
$k_{bw} = 133.677$,	$\kappa_{bv,b\phi} = 684.773$,	$\mu_{\ddot{a}w} = 0.817875$,
$k_{b\phi} = 16986.2$,	$\kappa_{bw,b\phi} = 625.955$,	$\mu_{\ddot{a}\phi} = 0.0151564$,
$\mu_{av,\ddot{a}v} = -79.1398$,	$\mu_{\dot{a}v,\dot{a}v} = -78.3826$,	$\mu_{bw,\ddot{a}w} = -0.662433$,
$\mu_{aw,\ddot{a}v} = 7.71894$,	$\mu_{\dot{a}w,\dot{a}w} = 0.649207$,	$\mu_{bw,\ddot{b}v} = 1.39161$,
$\mu_{aw,\ddot{a}w} = 0.107419$,	$\mu_{bv,\ddot{a}v} = 0.102172$,	$\mu_{bw,\ddot{b}\phi} = -0.0011083$,
$\mu_{a\phi,\ddot{a}v} = -0.000984119$,	$\mu_{bv,\ddot{a}w} = -0.662433$,	$\mu_{\dot{b}v,\dot{b}w} = 1.39161$,
$\mu_{a\phi,\ddot{a}w} = -0.0100401$,	$\mu_{bw,\ddot{a}v} = 0.102172$,	$\mu_{\dot{b}v,\dot{b}\phi} = 0.0011083$.
$\mu_{\dot{b}w,\dot{b}\phi} = -0.0011083$,		

References

[1] A.H. Nayfeh, P.F. Pai, *Linear and Nonlinear Structural Mechanics*, Wiley-Interscience, New York, 2004.
[2] A.H. Nayfeh, *Nonlinear Interactions*, Wiley, New York, 2000.
[3] M.R.M. Crespo da Silva, C.C. Glynn, Nonlinear flexural–flexural–torsional dynamics of inextensional beams: part I, equations of motion, *Journal of Structural Dynamics* 6 (4) (1978) 437–448.
[4] M.R.M. Crespo da Silva, C.C. Glynn, Nonlinear flexural–flexural–torsional dynamics of inextensional beams: part II, forced motions, *Journal of Structural Dynamics* 6 (4) (1978) 449–461.
[5] M.P. Cartmell, Simultaneous combination resonances in a parametrically excited cantilever beam, *Strain* (1987) 117–126.
[6] H.N. Arafat, A.H. Nayfeh, Char-Ming Chin, Nonlinear nonplanar dynamics of parametrically excited cantilever beams, *Nonlinear Dynamics* 15 (1998) 31–61.
[7] P. Malatkar, Nonlinear Vibrations of Cantilever Beams and Plates, PhD Thesis, Blacksburg, Virginia, 2003.
[8] A. Tondl, T. Ruijgrok, F. Verhulst, R. Nagergoj, *Autoparametric Resonance in Mechanical Systems*, Cambridge University Press, Cambridge, 2000.
[9] D. Sado, Energy transfer in nonlinearly coupled oscillators with two degrees of freedom, Mechanika, Vol. 166, Warsaw University of Technology Publisher, Warsaw, 1997 (in Polish).
[10] B. Balachandran, A.H. Nayfeh, Nonlinear motion of beam-mass structure, *Nonlinear Dynamics* 1 (1990) 39–61.
[11] A.H. Nayfeh, B. Balachandran, M.A. Collbert, An Experimental investigation of complicated responses of a two-degree-of-freedom structure, *Transactions of the ASME* 56 (1989) 960–966.
[12] A.H. Nayfeh, L.D. Zavodney, Experimental observation of amplitude- and phase-modulated responses of two internally coupled oscillators to a harmonic excitation, *Transactions of the ASME* 55 (1988) 706–710.
[13] J.W. Roberts, M.P. Cartmell, Forced vibration of a beam system with autoparametric coupling effects, *Strain* (1984) 117–126.
[14] M.P. Cartmell, J.W. Roberts, Simultaneous combination resonances in an autoparametrically resonant system, *Journal of Sound and Vibration* 123 (1) (1988) 81–101.
[15] M.P. Cartmell, The equations of motion for a parametrically excited cantilever beam, *Journal of Sound and Vibration* 143 (3) (1990) 395–406.
[16] S.L. Bux, J.W. Roberts, Non-linear vibratory interactions in systems of coupled beams, *Journal of Sound and Vibration* 104 (3) (1986) 497–520.
[17] D.I.M. Forehand, M.P. Cartmell, On the derivation of equations of motion of parametrically excited cantilever beam, *Journal of Sound and Vibration* 245 (1) (2001) 165–177.
[18] J. Warminski, M. Bochenski, Nonlinear vibrations of the autoparametrically coupled beam structure. *Proceedings of the Eighth Conference on Dynamical Systems—Theory and Applications*, Lodz, Poland, 2005, pp. 827–832.